Directed differentiation of mouse pluripotent stem cells into functional lung-specific mesenchyme

Andrea B. Alber[1,2], Hector A. Marquez[1,2], Liang Ma[1,2], George Kwong[1,2], Bibek R. Thapa[1,2], Carlos Villacorta-Martin[1], Jonathan Lindstrom-Vautrin[1], Pushpinder Bawa[1], Yongfeng Luo[3], Laertis Ikonomou[4,5], Wei Shi[3], Darrell N. Kotton[1,2*]

[1]Center for Regenerative Medicine of Boston University and Boston Medical Center, Boston, MA 02118, USA

[2]The Pulmonary Center and Department of Medicine, Boston University School of Medicine, Boston, MA 02118, USA

[3]Department of Surgery, Children's Hospital Los Angeles, Keck School of Medicine, University of Southern California, Los Angeles, CA 90027, USA

[4]Department of Oral Biology, School of Dental Medicine, University at Buffalo, Buffalo, NY 14260, USA

[5]Division of Pulmonary, Critical Care and Sleep Medicine, Department of Medicine, Jacobs School of Medicine and Biomedical Sciences, University at Buffalo, Buffalo, NY 14215, USA

*Corresponding author (dkotton@bu.edu)

Abstract

The successful generation of endodermal, ectodermal, and most mesodermal lineages from pluripotent stem cells has resulted in basic discoveries and regenerative medicine clinical trials of cell-based therapies. In contrast, the derivation of tissue-specific mesenchyme via directed differentiation in vitro has markedly lagged, due in part to a limited understanding of the signaling pathways regulating in vivo mesenchymal development and a lack of specific markers or reporters able to purify such lineages. The derivation of lung-specific mesenchyme is a particularly important goal since this tissue plays important roles in lung development and respiratory disease pathogenesis. Here we generate a mouse induced pluripotent stem cell (iPSC) line carrying a lung-specific mesenchymal reporter/lineage tracer facilitating the tracking and purification of engineered lung-specific mesenchyme. We identify the key signaling pathways (RA and Shh) necessary to specify lung mesenchyme from lateral plate mesodermal precursors and find that mouse iPSC-derived lung mesenchyme (iLM) expresses the molecular and functional phenotypes of primary developing lung mesenchyme. Purified iLM can be recombined with separately engineered lung epithelial progenitors, self-organizing into 3-dimensional organoids featuring significantly augmented structural complexity and lineage purity, including interacting juxtaposed layers of epithelium and mesenchyme. Co-culture with iLM increases the yield of lung epithelial progenitors and impacts epithelial and mesenchymal differentiation programs, suggesting functional epithelial-mesenchymal crosstalk. Our iPSC-derived population thus expresses key features of developing lung mesenchyme, providing an inexhaustible source of cells for studying lung development, modeling diseases, and developing therapeutics.

Introduction

The lung mesenchyme plays important roles in lung development and disease, yet knowledge is limited about the biology of lung mesenchymal progenitors, or how they initiate disease. In the mouse, lineage specification of the respiratory mesenchyme from splanchnic mesodermal precursors has been reported to occur around embryonic day (E) 9-9.5, a process coordinated through bi-directional endodermal-mesodermal signaling interactions[1–4]. Mouse models have helped to identify several key regulators potentially involved in lung mesenchyme specification and differentiation, such as Retinoic Acid (RA), Wnt/b-catenin, Sonic hedgehog (SHH), and BMP4[1,3,5–14]. However, our understanding of early lung mesenchyme specification and differentiation in the mouse is still limited, and how the lung mesenchyme is specified during human development is unknown.

Complementing animal models, induced pluripotent stem cell (iPSC) or embryonic stem cell (ESC)-derived lineages have emerged as powerful tools to study both development and disease, since these in vitro models allow easy experimental manipulation and provide an unlimited source of material[15,16]. iPSCs/ESCs have the potential to generate any lineage of interest in vitro by directed differentiation, i.e. the in vitro recapitulation of the sequence of in vivo developmental milestones by stepwise addition of growth factors or small molecules to stimulate key developmental signaling pathways. Our lab and others have established protocols for the directed differentiation of both mouse and human iPSC/ESCs into Nkx2-1+ lung epithelial progenitors, as well as towards more mature distal and proximal epithelial respiratory lineages[17–28]. In contrast, only two previous studies have attempted to generate lung-specific mesenchyme

by directed differentiation through a mesodermal progenitor[2,9]. While these studies have found an upregulation of mesenchymal markers by RT-qPCR in bulk cell extracts, they lacked specific reporters for cell tracking or purification, leaving unanswered questions about the efficiency of the differentiation protocol and the transcriptomic similarity of in vitro differentiated cells to primary lung mesenchyme.

A potential alternative approach to directed differentiation through a mesodermal progenitor state is the co-development of lung mesenchymal progenitors during in vitro differentiation of lung epithelial progenitor cells. Mouse lung epithelial differentiation protocols do not yield 100% differentiation efficiency, and thus might also contain non-epithelial lineages, such as mesodermal progenitors. Thus, co-development might occur when differentiating lung epithelial cells provide the signals necessary to specify lung mesenchyme from these mesodermal progenitor cells and vice versa. For example, we previously differentiated a lung epithelial-specific Nkx2-1^{mCherry} reporter mouse ESC line into mCherry+ lung epithelium and observed emergence of early lung mesenchymal markers enriched in Nkx2-1^{mCherry}- cells, implying co-development of both lineages[27]. Similarly, the emergence of human cells expressing general mesenchymal markers has been observed as a “by-product” of epithelial differentiation when using directed differentiation protocols without sorting for the epithelial progenitors of interest[17,29,30]. However, it remains unclear whether these mesenchymal cells can be classified as lung-specific mesenchyme, since no lung mesenchyme-specific reporters were available for use in these studies.

Importantly, several lines of evidence have suggested that embryonic mesenchyme is tissue-specific. Using tissue "recombinants", i.e. ex vivo cultures of embryonic epithelium mechanically combined with mesenchymal tissues, a study by Shannon has shown that recombining tracheal (i.e. proximal) epithelium with distal lung mesenchyme induced branching and expression of distal epithelial markers, while recombining lung (i.e. distal) epithelium with tracheal mesenchyme leads to the formation of cystic structures and expression of proximal epithelial markers[31]. This demonstrates that embryonic mesenchyme can determine region-specific epithelial identity and suggests different underlying gene expression profiles between region-specific embryonic mesenchymes. Supporting these early findings, Han et al. recently performed single cell RNA sequencing (scRNA-seq) of multiple organs of the early embryonic foregut and found specific transcriptional signatures for mesenchymes of each organ[2], highlighting the importance of generating tissue-specific mesenchyme as opposed to generic mesenchymal cells when using in vitro approaches to study development and disease.

While previous attempts to generate, track, and purify lung-specific mesenchyme have been limited by the lack of specific reporters or markers, this hurdle has been surmounted recently by the development of an in vivo lineage tracer/reporter system based on a lung mesenchyme-specific enhancer region in the *Tbx4* gene. While the *Tbx4* locus and transcript are more broadly expressed, this enhancer region appears to be selectively active in the developing lung mesenchyme and is evolutionarily conserved among multiple air-breathing species including mouse and human[32]. Zhang et al. and Kumar et al. have both successfully generated lung

mesenchyme-specific lineage tracing and reporter mice using this *Tbx4* lung enhancer element[33,34], providing invaluable tools to study early lung mesenchyme development.

Here we engineer iPSCs derived from a Tbx4 lung enhancer reporter/tracer mouse to develop a protocol for the directed differentiation of iPSCs into early lung mesenchyme. These iPSC-derived lung mesenchymal progenitors share transcriptional similarity with primary mouse embryonic lung mesenchyme and are competent to differentiate into more mature mesenchymal lineages. We assess the functional capacity of these engineered lung mesenchymal progenitors by generating 3-dimensional recombinant lung organoids composed of juxtaposed layers of separately derived engineered lung mesenchyme and engineered lung epithelium. We find that recombination appears to augment lung epithelial lineage specification and yield while impacting the molecular phenotypes of both lineages, suggesting functional epithelial-mesenchymal crosstalk in a multilineage lung organoid model system.

Results

Lung mesenchyme can be generated in vitro by directed differentiation of mouse iPSCs via lateral plate mesodermal intermediates

To develop a putative lung mesenchyme-specific in vitro fluorescent reporter/tracer system able to track and quantify the acquisition of early lung mesenchymal fate, we sought to generate an iPSC line from mice that we previously engineered to provide transgenic spatio-temporal lineage tracing of lung mesenchyme[34]. These triple transgenic mice carry an rtTA/LacZ encoding cassette under regulatory control of a *Tbx4* lung-specific enhancer, a Tet-responsive Cre recombinase, and

a fluorescent mTmG cassette (Tbx4-rtTA; TetO-Cre; mTmG, hereafter "Tbx4-LER"), enabling inducible green fluorescence lineage tracing specifically of embryonic lung mesenchymal cells, without tagging of mesenchyme in other tissues in vivo[34] (Figure 1a). To ensure that GFP tagging of primordial lung mesenchyme in these mice is specific and visible at the time of initial lung budding, a time point earlier than we have previously examined[34], we administered doxycycline (dox) to Tbx4-LER mice from embryonic day (E) E6.5 to E10 and observed GFP fluorescence at E10 in the developing primordial lung mesenchyme (Figure 1a).

Next, we reprogrammed tail tip fibroblasts from a triple transgenic Tbx4-LER mouse, generating iPSCs that exhibited a normal karyotype and expressed pluripotency markers (Supplementary Figure 1a-e). To test their mesenchymal competence, we first differentiated iPSCs into lateral plate mesoderm, the precursor tissue from which lung mesenchyme is thought to originate during early development. We used our previously published serum-free directed differentiation protocol[35] producing KDR+ putative mesodermal cells in 5 days in response to WNT3A, BMP4, and Activin A with similar efficiency to previously published studies[35,36] (Figure 1b-c, Supplementary Figure 1f-g). Consistent with our prior publication[35], sorted KDR+ day 5 cells were highly enriched in lateral plate mesoderm marker *Foxf1*, and expressed only low levels of paraxial and intermediate mesoderm markers *Tbx6* and *Pax2* (Figure 1c). In the first 5 days of differentiation, no Tbx4-LER activation was observed in the presence of dox (Supplementary Figure 1h), suggesting that day 5 iPSC-derived lateral plate mesoderm is not yet specified to a lung mesenchymal fate in these conditions.

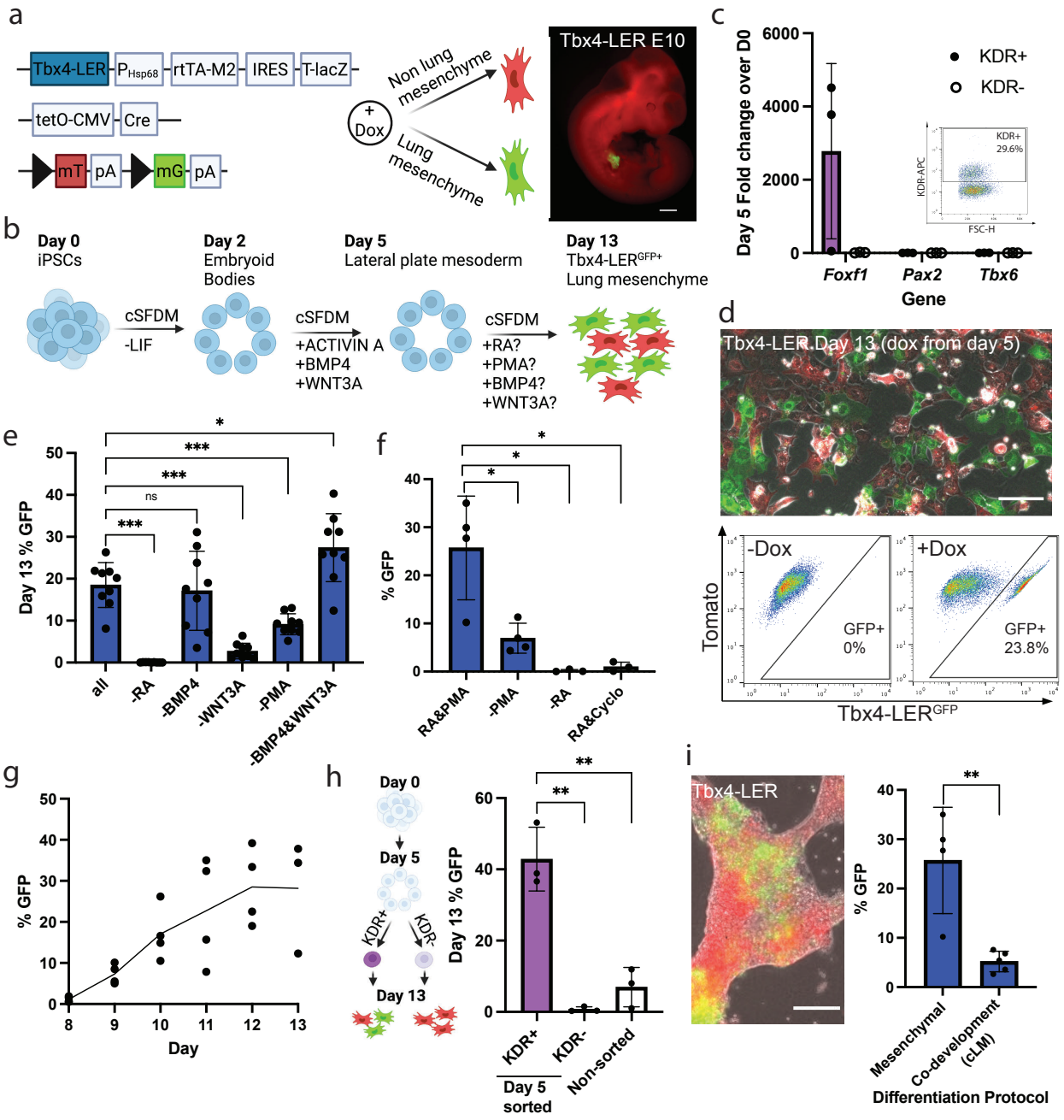

Figure 1: In vitro differentiation of iPSCs towards the lung mesenchyme lineage through a mesodermal progenitor.

a: Schematic of the triple transgenic *Tbx4* lung enhancer reporter/tracer (LER) line, and image of an E10 embryo (dox from E6.5-E10). Scale bar = 0.5 mm. **b**: Protocol for the directed differentiation of iPSCs into lung mesenchyme through a mesodermal progenitor. cSFDM = complete serum-free differentiation medium, LIF = Leukemia inhibitory factor. **c**: Fold change expression relative to day 0 iPSCs of *Foxf1* (lateral plate mesoderm), *Pax2* (intermediate mesoderm) and *Tbx6* (paraxial mesoderm) in KDR+/- sorted cells on day 5 of differentiation. N = 3. **d**: Representative image and flow cytometry plot showing expression of GFP (green) in the Tbx4-LER iPSC line on day 13 of differentiation. Red=Tomato in non-recombined (untraced) cells. Scale bar = 100 µm.

e: Percentage of GFP+ cells on day 13 of differentiation. Day 5-13 medium contained either all 4 factors (RA, PMA, BMP4 and WNT3A), or one or two factors were removed at a time. Dox was kept in the medium from day 5 on. N=9. **f**: Percentage of GFP+ cells on day 13 of differentiation in RA&PMA medium, upon removal of either RA or PMA, as well as upon addition of the Hedgehog inhibitor Cyclopamine. Dox was kept in the medium from day 5 on. N ≥ 3. **g**: Percentage of GFP+ cells over time, quantified every day from day 5-13. Dox was kept in the medium from day 5 on. N ≥ 3. **h**: Percentage of GFP+ cells on day 13 of differentiation in RA&PMA medium after sorting for KDR+/- on day 5 of differentiation. N = 3. **i**: Representative image showing reporter activation on day 13 of lung epithelial differentiation and percentage of GFP+ cells in the mesenchymal versus epithelial (i.e. co-development, cLM) differentiation protocol. Dox was kept in the medium from day 5 on in the mesenchymal differentiation protocol, and from day 6 (anterior foregut endoderm stage) on in the epithelial (co-development) protocol. Scale bar = 100 µm. N = 4 for "Mesenchymal", N = 5 for "Co-development".
All bars show mean ± sd. *p<0.05, **p<0.01, ***p<0.001, ns = non-significant, as determined by unpaired, two-sided Student's t test.

In order to specify lung mesenchyme from lateral plate mesoderm cells, we tested the combinatorial effects of 4 growth factors and small molecules (RA, BMP4, WNT3A, and purmorphamine [PMA]) selected to stimulate developmental pathways with suggested roles in lung mesenchyme formation published in vivo[2]: Retinoic Acid (RA), BMP, canonical Wnt, and Hedgehog (Hh) signaling, respectively. These 4 factors added beginning at day 5 together with dox resulted in 18.5 ± 5% of cells activating the Tbx4-LER^{GFP} lineage trace by day 13 (Figure 1d-e). To identify which of these factors is required for Tbx4-LER activation, we removed 1 or 2 factors at a time (Figure 1e), finding that RA was absolutely required for Tbx4-LER^{GFP} induction, whereas BMP4 was dispensable and removing both BMP4 and WNT3A resulted in the highest (27.4 ± 7.6%) Tbx4-LER^{GFP} efficiency, suggesting that stimulated RA together with Hh signaling represents a minimal combination required for efficient Tbx4-LER activation. To further determine the differential effects of RA and Hh signaling on lung mesenchyme differentiation efficiency, we removed either factor from the differentiation medium. Removing PMA significantly decreased

the percentage of Tbx4-LER^{GFP}+ cells, but still generated an average of 6.9 ± 2.7% of Tbx4-LER^{GFP}+ cells (Figure 1f). In contrast, removing RA led to a complete lack of Tbx4-LER^{GFP}+ cells, confirming that RA signaling is necessary to specify lung mesenchyme from lateral plate mesoderm (Figure 1f). Finally, adding the Hh inhibitor Cyclopamine to RA-containing differentiation medium completely abolished Tbx4-LER^{GFP} activation (Figure 1f), suggesting that combinatorial RA together with Hedgehog signaling promotes lung mesenchymal differentiation.

Having established a defined minimal medium (RA and PMA) for Tbx4-LER activation, we profiled the temporal dynamics of Tbx4-LER^{GFP} induction, adding dox from day 5 of differentiation on, and scoring Tbx4-LER^{GFP} efficiency daily until day 13. The percentage of Tbx4-LER^{GFP}+ cells increased from day 9 to day 12 of differentiation (Figure 1g). Furthermore, sorting day 5 KDR+ cells enriched for GFP competence, yielding an average of 40% of Tbx4-LER^{GFP}+ cells on day 13, whereas KDR- sorted cells were completely depleted of GFP competence, suggesting that only KDR+ lateral plate mesodermal cells serve as precursors for Tbx4-LER^{GFP}+ lung mesenchyme in our model system (Figure 1h).

Previous studies have demonstrated that it is possible to “co-develop” both mesodermal and endodermal epithelial lineages together in the same differentiation medium when using directed lung epithelial differentiation protocols[17,27,29,30]. Hence, we aimed to investigate whether Tbx4-LER^{GFP}+ lung mesenchyme can also be derived by co-development during directed lung endodermal/epithelial differentiation as an alternative approach to directed differentiation via a mesodermal progenitor. We used our published lung epithelial differentiation protocol[27,37] to

differentiate the Tbx4-LER iPSC line into the Nkx2-1+ lung epithelial progenitor stage (Figure Supplementary Figure 1i) and by day 13 observed the emergence of both Nkx2-1+ epithelial cells as expected (data not shown), as well as an average of 5.2 ± 1.9% of Tbx4-LER^{GFP}+ cells (Figure 1i), suggesting that co-development of lung mesenchyme ("cLM") and epithelium is indeed feasible. However, since lung mesenchymal differentiation by co-development was significantly less efficient than directed lung mesenchymal differentiation through a lateral plate mesoderm progenitor state ("mesenchymal"; Figure 1i), we largely focused on directed lung mesenchymal differentiation through a mesodermal progenitor for further characterization and downstream applications.

Induced lung mesenchyme is transcriptionally similar to primary embryonic lung mesenchyme

Next, we used single cell RNA sequencing (scRNA-seq) to compare the molecular phenotypes of Tbx4-LER^{GFP}+ cells and Tbx4-LER^{GFP}- cells generated by directed lung mesenchymal differentiation through a mesodermal progenitor state. For a control comparator we also profiled primary mouse embryonic lung mesenchyme from embryonic day (E) 12.5, (hereafter referred to as "primary") (Figure 2a). By Louvain clustering we found that iPSC-derived cells largely segregated into two distinct cell clusters, one almost exclusively consisting of Tbx4-LER^{GFP}+ cells (cluster 1; Figure 2b), the second mostly consisting of Tbx4-LER^{GFP}- cells with a minor subset composed of GFP+ cells (cluster 2, Figure 2b). Primary lung mesenchymal cells formed two distinct clusters: a main mesenchymal cluster (cluster 3) and an additional minor cluster annotated as mesothelial cells based on canonical markers (cluster 4, Fig 2B, Supplementary Figure 2a-b). Both the iPSC-derived cluster 1 and the major primary mesenchymal cluster 3 expressed lung mesenchymal

markers, such as *Tbx4*, *Foxf1*, and Hh targets (*Gli1*, and *Hhip*), as well as *Pdgfra*. In contrast most of these markers were expressed at lower levels in iPSC-derived cluster 2 (Supplementary Figure 2c). Analysis of the combined expression of a list of 13 lung mesenchymal markers (Supplementary Table 1) known from the literature including *Foxf1*, *Tbx4/5*, *Wnt2/2b* and Hh targets[2,5,7,12,14,38,39] (further referred to as LgM gene set), as well as a published set consisting of 61 genes (Supplementary Table 1) found to be enriched in E9.5 lung mesenchyme[2] further showed that cluster 1 iPSC-derived cells are more transcriptionally similar to primary E12.5 lung mesenchyme than iPSC-derived cluster 2 cells (Figure 2c). In addition, we also analyzed the expression of both gene sets in co-developed lung mesenchyme (cLM) and found lower expression levels of these gene signatures in cLM compared to iPSC-derived Tbx4-LER^{GFP}+ cells generated through directed mesenchymal differentiation (Supplementary Figure 2d), suggesting that directed differentiation results in superior engineered lung mesenchymal cells, at least in these protocols. Next, focusing on differences between iPSC-derived cluster 1 cells and primary cells, we found *Wnt2* to be more highly expressed in primary cells, along with canonical Wnt signaling target genes, such as *Lef1* and *Snai1/2* (Supplementary Figure 2a, 2c), suggesting that activation of the Wnt signaling pathway is lower in cluster 1 cells in these conditions compared to primary embryonic lung mesenchyme. Importantly, we found that both iPSC-derived cluster 1 mesenchyme and primary embryonic lung mesenchyme expressed only low to undetectable levels of markers for embryonic non-lung foregut mesenchyme such as *Wnt4/Msc* (esophageal) and *Barx1* (gastric, Figure 2d)[2] whereas the majority of iPSC-derived cluster 2 cells expressed high levels of the esophageal mesenchymal marker Wnt4. Finally, in cluster 1 cells we observed low to undetectable levels of more mature mesenchymal lineage markers, such as *Acta2/Myh11*

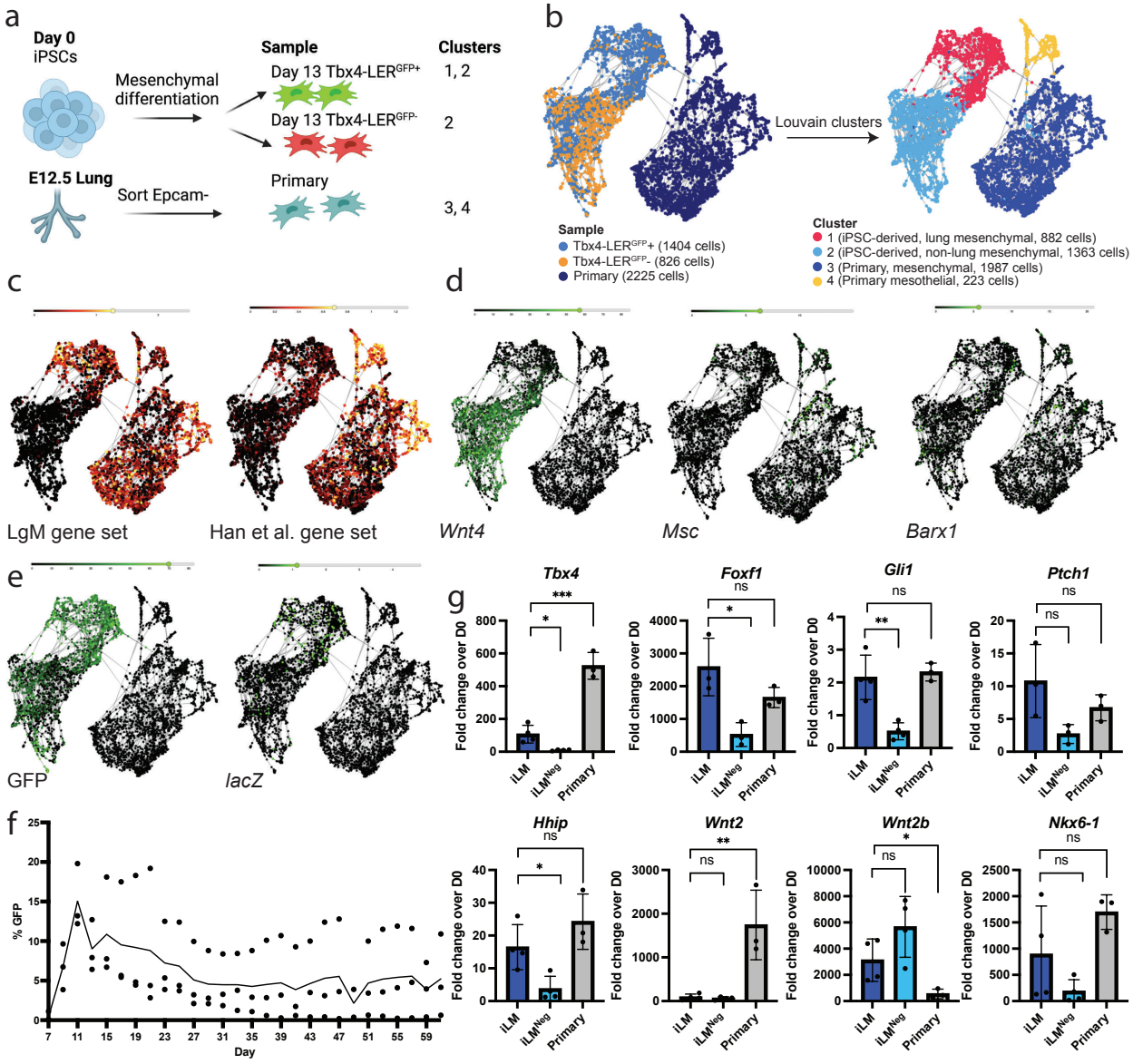

Figure 2: Transcriptomic characterization of iPSC-derived lung mesenchyme compared to primary embryonic lung mesenchyme.

a: Schematic of the samples included in scRNA-seq dataset. **b**: SPRING plots showing the samples (left panel) included in scRNA-seq analysis, as well as the clusters (right panel) identified by Louvain clustering (resolution 0.1). Tbx4-LER^{GFP}+/- cells were collected on day 13 of differentiation, dox was added from day 5 on. Primary = E12.5 embryonic lung mesenchyme. **c**: SPRING plots showing the enrichment of a gene set of 13 embryonic lung mesenchyme markers known from the literature (LgM), and a set of 61 genes enriched in E9.5 lung mesenchyme published by Han et al., 2021. **d**: SPRING plots showing expression of embryonic esophageal markers *Wnt4* and *Msc*, as well as embryonic gastric marker *Barx1* in iPSC-derived and primary cell clusters. **e**: SPRING plot showing expression of GFP and LacZ in iPSC-derived and primary cell clusters.

f: Dox induction time-course showing percentage of GFP+ cells over time, with dox added 2 days before each day of quantification. N = 3. **g**: RT-qPCR showing fold change expression relative to day 0 iPSCs of lung mesenchyme markers in induced lung mesenchyme (iLM) and iLM^{Neg} cells compared to primary lung mesenchyme from E12.5 embryos. Tbx4-LER^{GFP}+/- cells were collected on differentiation day 13 and dox was added from day 5 on. N ≥ 3. Bars show mean ± sd. *p<0.05, **p<0.01, ***p<0.001, ns = non-significant, as determined by unpaired, two-sided Student's t test.

(smooth muscle), *Plin1/Pparg* (adipocytes/lipofibroblasts), and *Col2a1* (chondrocytes) (Supplementary Figure 2e), suggesting that iPSC-derived cluster 1 cells at this time point express an early lung mesenchymal progenitor molecular phenotype without significant maturation.

Since a minor subset of Tbx4-LER^{GFP}+ lineage traced cells clustered together with Tbx4-LER^{GFP}- cells (cluster 2) and were not enriched in lung mesenchymal markers (Figures 2b-c, e), we considered the possibility that some GFP lineage-traced cells undergoing directed lung mesenchymal differentiation only transiently acquire a lung mesenchymal progenitor state, with subsequent loss of lung specific mesenchymal marker expression despite persistence of the GFP lineage trace. We anticipated that GFP+ cells that expressed an active developing lung mesenchymal progenitor program could be distinguished based on either short term dox induced GFP lineage tracing or based on expression of the lacZ reporter driven by the transgenic Tbx4 lung enhancer (Figure 1a). Indeed, we found the subpopulation of GFP+ lineage traced cells that expressed high levels of lung mesenchymal markers were also enriched in transcripts encoding the lacZ reporter, whereas those GFP+ cells in cluster 2 did not express lacZ, suggesting they had lost their prior lung mesenchymal program as indicated by loss of Tbx4 lung-specific enhancer activity (Figure 1a, 2e). We thus performed a time-course experiment where we differentiated cells using the lung mesenchymal differentiation protocol and quantified the percentage of Tbx4-

LER^{GFP}+ cells every 2 days until day 61, while only adding dox 2 days prior to each analysis. We found that Tbx4-LER^{GFP} activation peaks at day 11 of differentiation and subsequently decreases to lower levels (Figure 2f), consistent with the hypothesis that the lung mesenchymal progenitor state acquired during directed lung mesenchymal differentiation is transient.

Having demonstrated that iPSC-derived cells produced by our protocol and expressing an active Tbx4 lung specific enhancer element are enriched in lung mesenchymal markers we thus annotated Tbx4-LER^{GFP}+ cells as putative induced lung mesenchyme (hereafter "iLM") and Tbx4-LER^{GFP}- cells as "iLM^{neg}". We sought to validate the expression of a selected subset of these lung mesenchymal markers in iLM, iLM^{Neg}, and primary E12.5 lung mesenchymal cells by RT-qPCR (Figure 2g, Supplementary Figure 2f). We found significant enrichment in *Tbx4, Foxf1, Gli1*, and *Hhip* in iLM vs iLM^{Neg} cells. Additional lung mesenchymal markers (*Nkx6-1, Ptch1*) were highly expressed in iLM cells at levels no different from primary controls, and their expression was also detected in and not significantly different from iLM^{Neg} cells. While *Wnt2* expression was significantly lower in iLM cells compared to E12.5 lung mesenchyme, the expression of *Wnt2b* was significantly higher. Finally, we detected no significant differences in the expression of the general mesenchymal markers *Pdgfra* and *Col1a1*, or the smooth muscle marker *Acta2* between iLM cells and our primary control. In conclusion, the majority of assessed mesenchymal genes were expressed at similar levels to primary control cells, further confirming observations from our scRNA-seq dataset, and indicating that iPSC-derived engineered lung mesenchyme purified based on Tbx4-LER activation shares transcriptomic similarity with primary embryonic lung mesenchyme.

Induced lung mesenchymal progenitors are competent to differentiate into more mature mesenchymal lineages

We next sought to investigate whether iLM cells are competent to differentiate into more mature mesenchymal lineages (Figure 3a). To further differentiate iLM, we sorted day 13 Tbx4-LER^{GFP}+ cells and re-plated them in a smooth muscle differentiation medium that we previously published[35]. After 4 days, cells elongated and significantly upregulated expression of smooth muscle markers *Acta2* and *Tagln*, while downregulating expression of the early lung mesenchymal marker *Tbx4* (Figure 3b-d). Conversely, we found an increased deposition of lipid droplets when culturing iLM cells in adipogenic medium, as compared to parallel control cultures of iLM cells continued in mesenchymal medium (Figure 3e). In contrast, iLM cells by day 7 had lost vascular endothelial differentiation competence. When day 5 iPSC-derived lateral plate mesodermal cells were re-plated in VEGF-containing endothelial medium, the endothelial marker CDH5 was later expressed on the surface of 20% of the cellular outgrowth, whereas differentiating unsorted Tbx4-LER cells transferred to the same endothelial medium on day 7 gave rise to few (<5%) CDH5+ endothelial cells when analyzed after 2-8 more days in culture, and none of these emerging CDH5+ cells were Tbx4-LER^{GFP}+ (Figure 3f). This suggests rapid loss of endothelial competence during directed lung mesenchymal differentiation after the lateral plate mesoderm state. These findings are in agreement with Zhang et al., who showed that developing Tbx4-LER^{GFP}+ cells rapidly lose endothelial competence in vivo by E11.5, while their competence to differentiate into other mesenchymal lineages is maintained until later embryonic time-points[34].

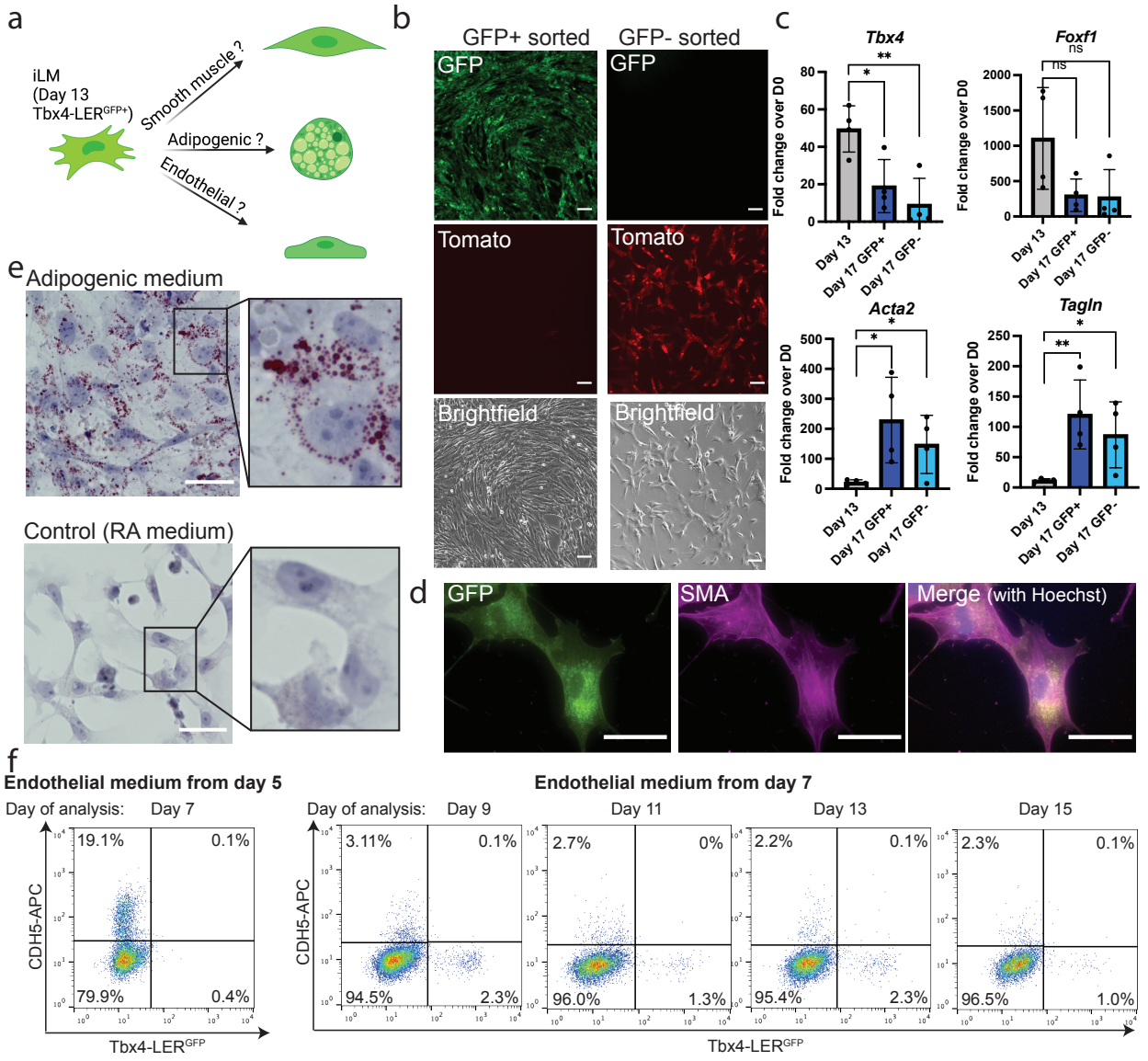

Figure 3: Induced lung mesenchymal progenitors are competent to differentiate towards more mature mesenchymal lineages.

a: Schematic of mesenchymal lineage differentiations performed. **b**: Representative image showing morphology of Tbx4-LER^{GFP}+ vs Tbs4-LER^{GFP}- cells sorted on day 13 of differentiation and subsequently cultured in smooth muscle differentiation medium for 4 days. Scale bars = 100 µm. **c**: RT-qPCR showing fold change expression relative to day 0 iPSCs of early lung mesenchyme markers *Tbx4* and *Foxf1*, as well as smooth muscle markers *Acta2* and *Tagln* on day 13 of differentiation (D13 = day 13 unsorted cells), and after 4 days of culture in smooth muscle differentiation medium (D17 GFP+/- = Tbx4-LER^{GFP}+/- cells sorted on day 13 and subsequently cultured in smooth muscle medium for 4 days). N = 4, Bars show mean ± sd. *p<0.05, **p<0.01, ***p<0.001, ns = non-significant, as determined by unpaired, two-sided Student's t test. **d**: Immunofluorescence image showing expression of GFP and smooth muscle actin (SMA) in Tbx4-LER^{GFP}+ cells that were sorted on day 13 and cultured in smooth muscle medium for 4 days. Scale bars = 100 µm.

e: Oilred O and hematoxylin stain of cells sorted for Tbx4-LER^{GFP}+ on day 13 and cultured in adipogenic medium for 9 days. Control cells were kept in lung mesenchyme medium (cSFDM+RA). Scale bars = 100 µm. **f**: Flow cytometry analysis showing CDH5 cell surface expression after culture in endothelial medium (cSFDM+VEGF). Left panel: endothelial medium added on day 5 of differentiation, cells analyzed on day 7. Right panel: endothelial medium added on day 7 of differentiation and cells analyzed on days 9, 11, 13 and 15.

Induced lung mesenchyme forms 3-dimensional "recombinant" organoids when co-cultured with engineered lung epithelial progenitors

One of the key functions of developing lung mesenchyme in vivo is to closely interact with and signal to the developing lung epithelium. Thus, in order to investigate the functional competence of iLM, we established a lung epithelial-mesenchymal co-culture system (Figure 4a) where we separately differentiated our Tbx4-LER^{GFP} iPSC line into iLM cells, and a Nkx2-1^{mCherry} reporter ESC line[40] into an Nkx2-1+ lung epithelial progenitor state using our published protocol[27,37]. As noted above, in order to enrich for cells that have an activated Tbx4-LER reporter at the time of collection (see Figure 2e-f), we used only short term dox exposure, restricting the addition of dox to differentiation day 9-11, and collected Tbx4-LER^{GFP}+ cells on day 11 for all co-culture experiments. We purified lung epithelial and iLM derivatives by flow cytometry and plated them on top of a bed of 3D Matrigel in our previously published distal (alveolar) or proximal (airway) lung epithelial differentiation media[27,37] (Figure 4a). Co-cultured cells self-organized into 3-dimensional organoids (recombinants) with juxtaposed layers of Tbx4-LER^{GFP}+ lung mesenchyme and Nkx2-1^{mCherry}+ lung epithelium (Figure 4b-d). Distal and proximal cultures differed in morphology, with distal cultures showing a more lobular and proximal cultures showing a more cystic structure (Figure 4b-c). In contrast, Nkx2-1^{mCherry}+ lung epithelium co-cultured with mouse embryonic fibroblasts (MEFs, i.e. a non-lung mesenchymal cell type control) did not associate

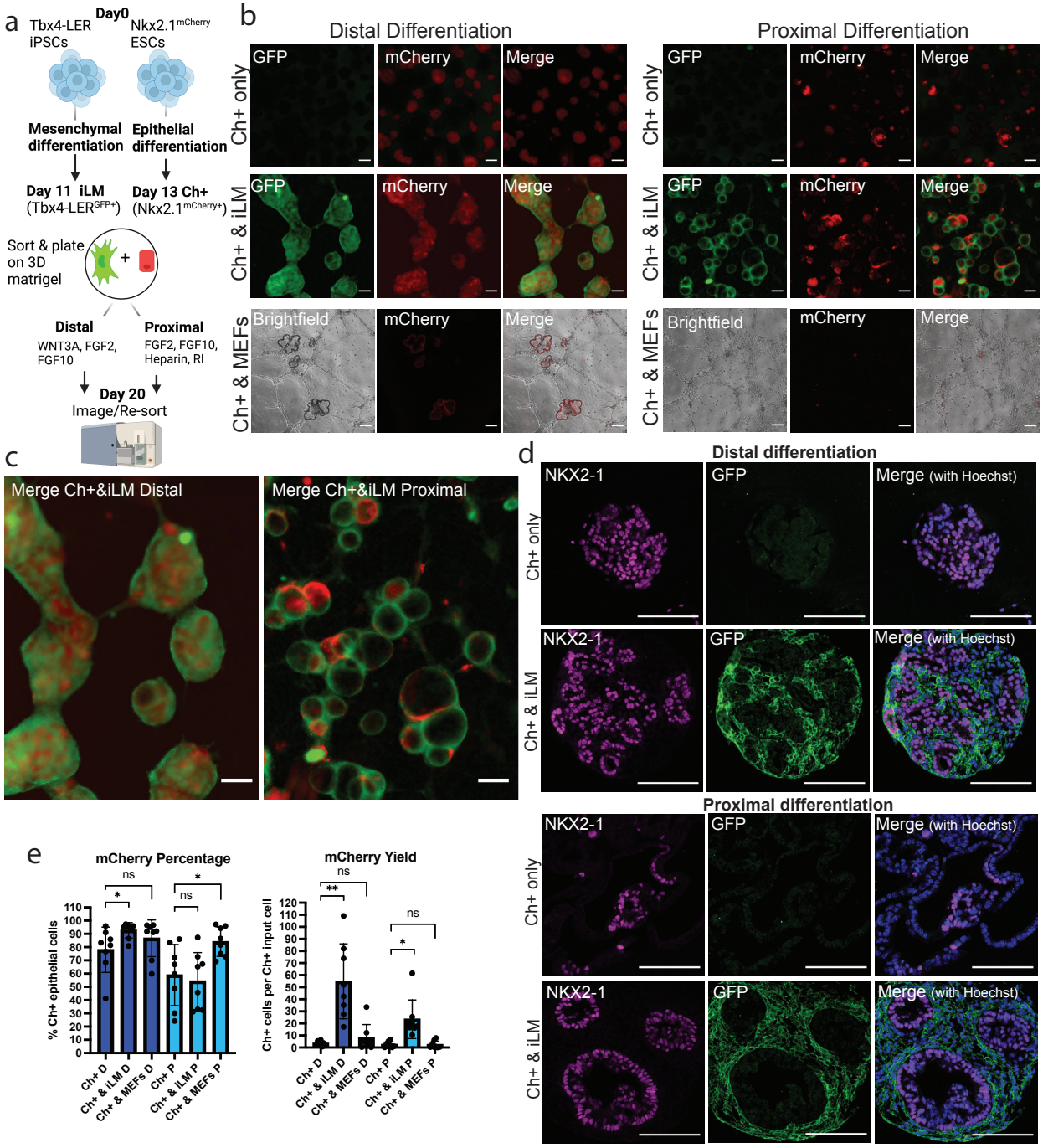

Figure 4: Co-culture of induced lung mesenchyme with Nkx2-1^{mCherry}+ lung epithelial progenitors leads to the formation of 3-dimensional organoids and increases yield of Nkx2-1^{mCherry}+ cells in distal and proximal epithelial differentiation conditions.

a: Schematic of lung epithelial-mesenchymal co-culture experiments. Nkx2.1^{mCherry} ESCs and Tbx4-LER iPSCs were differentiated separately using the lung epithelial or lung mesenchymal differentiation protocol. Day 11 Tbx4-LER^{GFP}+ (=iLM) and Day13 Nkx2-1^{mCherry}+ (Ch+) cells were then mixed at a 20:1 ratio and cultured for 7 days in either distal or proximal differentiation medium. **b**: Representative images of day 20 co-cultures. Day 13 Nkx2.1^{mCherry}+ (Ch+) cells were cultured in distal or proximal medium, either alone, with iLM cells or with a non-lung mesenchyme control (Mouse embryonic fibroblasts, MEFs). Scale bars = 200 µm.

c: Zoomed in versions of distal and proximal co-culture images shown in panel B. Scale bars = 200 µm. **d**: Immunofluorescence images showing expression of NKX2-1 and GFP in Nkx2-1^{mCherry}+ cells cultured in distal or proximal conditions alone or co-cultured with iLM for 1 week. Scale bars = 100 µm. **e**: Percentage of Nkx2.1^{mCherry}+ cells and yield (i.e. number of Nkx2.1^{mCherry}+ cells per day 13 Nkx2.1^{mCherry}+ input cell) for Nkx2.1^{Cherry}+ cells cultured alone, with iLM or with MEFs in distal or proximal medium. N = 8. Bars show mean ± sd. *p<0.05, **p<0.01, ***p<0.001, ns = non-significant, as determined by paired, two-sided Student's t test.

closely and showed poor outgrowth of Nkx2-1^{mCherry}+ cells, suggesting that co-culture with non-lung mesenchymal cells does not lead to 3D self-organization or detectable physical juxtaposition of the two lineages (Figure 4b). Re-sorting after co-culture to analyze the frequency and yield of each cell lineage revealed that co-culture with iLM significantly increased both the percentage and yield of Nkx2-1^{mCherry}+ epithelial cells after 1 week in distal differentiation medium, as compared to Nkx2-1^{mCherry}+ only culture controls (Figure 4e, Supplementary Figure 3a). Furthermore, co-culture with iLM significantly increased the yield of Nkx2-1^{mCherry}+ cells in proximal culture conditions compared to Nkx2-1^{mCherry}+ cells cultured alone, while co-culture with MEFs did not (Figure 4e, Supplementary Figure 3b).

Co-culture with induced lung mesenchyme affects lung epithelial differentiation programs

We next sought to determine whether co-culture with iLM might provide signals that impact the molecular phenotype of differentiating ESC-derived lung epithelial cells. Given that iLM resembles an early lung mesenchymal progenitor state, we speculated that co-culture with iLM might maintain Nkx2-1^{mCherry}+ cells in a less mature state compared to Nkx2-1^{mCherry}+ epithelial-only cultures. Indeed, RT-qPCR analysis of re-sorted cells indicated that Nkx2-1^{mCherry}+ cells co-cultured with iLM in distal medium expressed higher levels of early lung epithelial markers such as *Sox9* and *Etv5*, but lower levels of more mature distal epithelial lineage markers such as *Sftpc*,

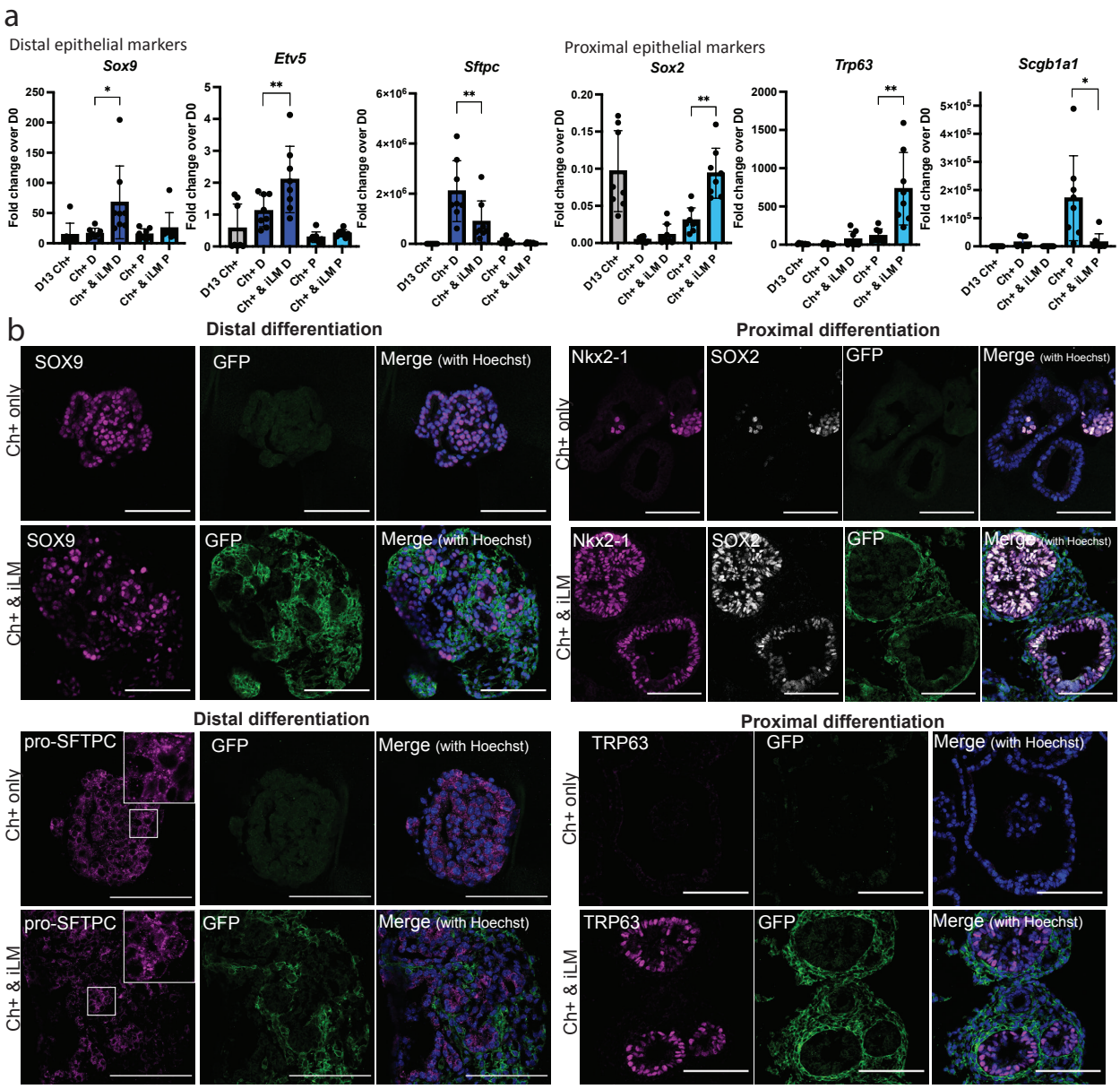

Figure 5: Co-culture with induced lung mesenchyme impacts the differentiation program of Nkx2-1^{mCherry}+ lung epithelial progenitors.

a: RT-qPCR data showing fold change expression relative to day 0 iPSCs of distal and proximal lung/airway markers in Nkx2-1^{mCherry}+ cells before (grey) and after co-culture in distal (dark blue) and proximal (light blue) medium. N = 8. Bars show mean ± sd. *p<0.05, **p<0.01, ***p<0.001, ns = non-significant, as determined by paired, two-sided Student's t test. **b**: Immunofluorescence images showing expression of distal and proximal epithelial markers of interest in Nkx2-1^{mCherry}+ cells cultured in distal or proximal conditions alone or co-cultured with iLM for 1 week. Scale bars = 100 µm.

Ager and *Hopx*, compared to Nkx2-1^{mCherry}+ cells cultured alone (Figure 5a, Supplementary Figure 4a). In proximal differentiation conditions, expression of airway markers known to arise early in development, such as *Sox2* and *Trp63* was increased in Nkx2-1^{mCherry}+ cells co-cultured with iLM compared to Nkx2-1^{mCherry}+ cells cultured alone. In contrast, markers that arise later in development, such as the club cell marker *Scgb1a1*, were decreased in Nkx2-1^{mCherry}+ cells co-cultured with iLM compared to Nkx2-1^{mCherry}+ cells cultured alone (Figure 5a, Supplementary Figure 4a). Nkx2-1^{mCherry}+ cells in all conditions tested were enriched for *Nkx2-1*, but expressed little to no thyroid marker *Pax8* or forebrain marker *Otx1* (Figure Supplementary Figure 4b), suggesting maintenance of lung-specific identity. Immunofluorescence further confirmed expression at the protein level of *Sox9*, *Sftpc*, *Sox2*, and *Trp63* and indicated that in recombinant cultures GFP lineage-traced iLM descendants surrounded and abutted the more centrally located lung epithelia expressing these markers (Figure 5b). Thus, our results suggest that co-culture with induced lung mesenchyme not only increases the yield of Nkx2-1^{mCherry}+ cells after culture in distal and proximal differentiation medium, but also affects the epithelial differentiation programs of their descendants.

Co-culture with induced lung mesenchyme can induce lung epithelial fate in non-lung epithelial progenitors

Having found that co-culture with iLM augments the percentage and yield of Nkx2-1^{mCherry}+ epithelial progenitors in distal differentiation conditions, we sought to determine whether iLM can also actively induce lung epithelial fate in ESC-derived endodermal cultures. We thus sorted day 13 Epcam+/Nkx2-1^{mCherry}- cells (i.e. epithelial cells that had not acquired a lung-specific fate

by day 13 of differentiation) and co-cultured them with iLM in distal differentiation medium (Figure 6a). The resulting recombinants self-assembled into 3D structures with similar morphology to recombinants of iLM with Nkx2-1^{mCherry}+ cells (Figure 6b). After 7 days, 82.0 ± 4.8 % of the previously Nkx2-1^{mCherry}- cells expressed mCherry (Figure 6c-d). In contrast, only 27.3 ± 14.6 % of Nkx2-1^{mCherry}- cells cultured in distal differentiation medium alone turned mCherry positive, and Nkx2-1^{mCherry}- cells co-cultured with MEF controls did not detectably expand in culture (Figure 6c-d). Re-sorting of post co-culture Nkx2-1^{mCherry}+ cells and RT-qPCR analysis revealed no differences in expression of lung epithelial lineage markers in the Nkx2-1^{mCherry}+ outgrowth from any sample, regardless of whether the cells were Nkx2-1^{mCherry}+ or Nkx2-1^{mCherry}- prior to co-culturing with iLM (Figure 6e).

Finally, to further investigate the functional capacity of iLM cells, we asked whether they can also be co-cultured with primary mouse alveolar epithelial type 2 (AT2) cells. Primary mouse AT2 cells have previously been grown in co-culture with primary mouse lung mesenchymal cells [41], but do not survive in culture in these conditions by themselves. We thus sought to co-culture iLM with primary mouse AT2 cells from an Sftpc-tdTomato lineage tracer mouse[42] (Figure 6f). We found that, similar to our co-cultures with engineered epithelial progenitors, AT2 cells co-cultured with iLM form 3D organoids with closely juxtaposed layers of mesenchyme and epithelium (Figure 6g). Co-cultured AT2 cells expressed pro-SFTPC (Figure 6g), indicating that AT2 cells maintain their fate. Thus, our data suggests that iLM can support outgrowth of primary AT2 cells.

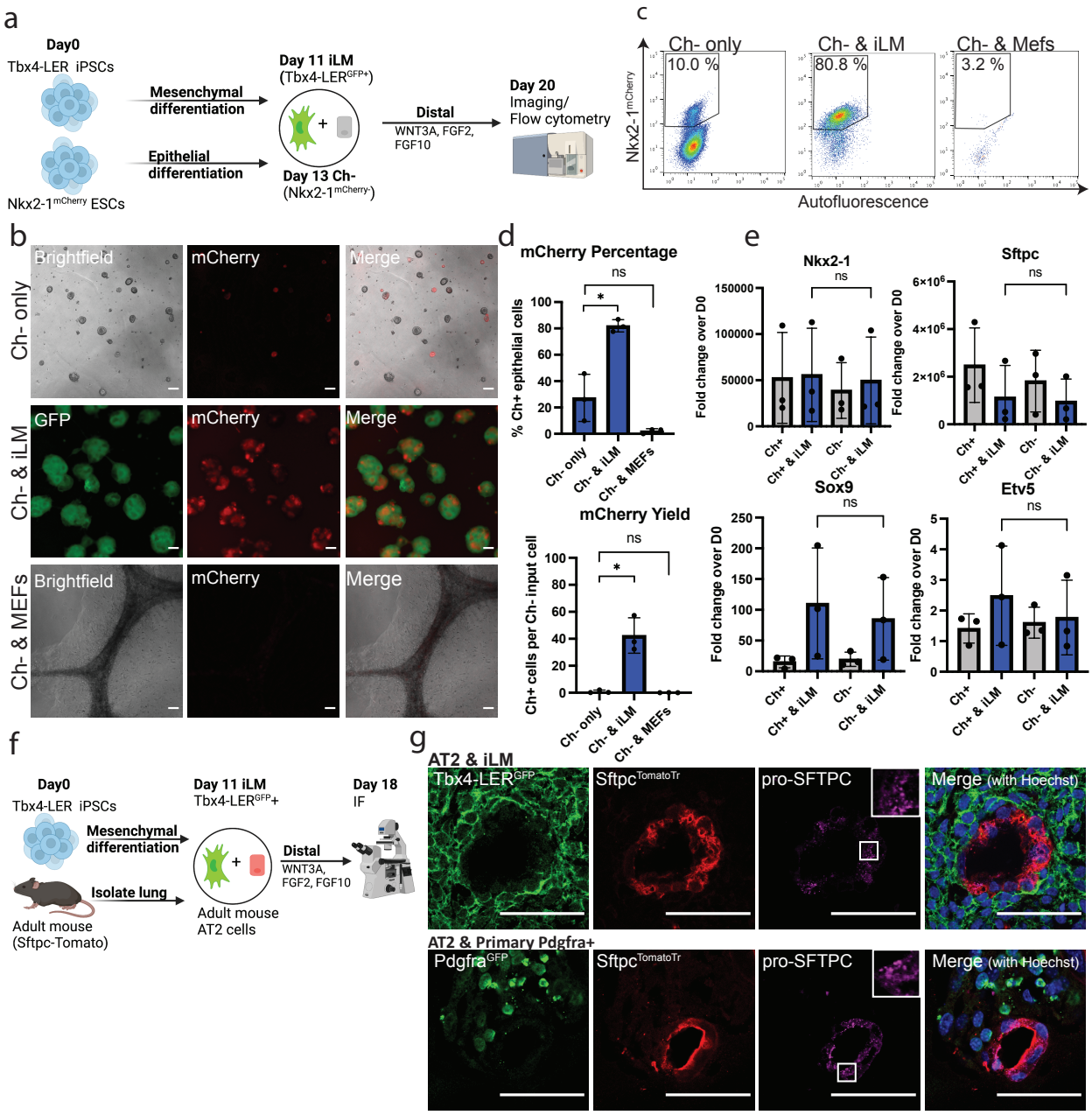

Figure 6: Co-culture with in vitro differentiated lung mesenchyme can induce lung epithelial fate in non-lung epithelial progenitors and can maintain primary AT2 cells.

a: Schematic of co-cultures with Nkx2-1^{mCherry}- day 13 cells. **b**: Representative images of co-cultures with Nkx2-1^{mCherry}- cells. Cells were sorted for Epcam+/mCherry- on day 13 of epithelial differentiation and cultured either alone, with iLM, or with non-lung mesenchyme (MEFs) in distal medium for 7 days. Scale bars = 200 µm. **c**: Representative flow cytometry plots showing percentage of Nkx2-1^{mCherry}+ cells for Nkx2-1^{mCherry}- cells cultured alone, with iLM or with MEFs in distal medium for 7 days. Cells were pre-gated for single cells, live cells, GFP- and Epcam+ cells. **d**: Percentage of Nkx2-1^{mCherry}+ cells and yield (i.e. number of Nkx2-1^{mCherry}+ cells per Day 13 Nkx2-1^{mCherry}- input cell) for Nkx2-1^{mCherry}- cells cultured either alone, with iLM, or with MEFs in distal medium for 7 days. N = 3.

e: Expression relative to day 0 iPSCs of distal lung markers in day 20 Nkx2-1^{mCherry}+ cells after distal culture. Day 13 Nkx2-1^{mCherry}+/- cells (Ch+/Ch-) were sorted on day 13 of differentiation and cultured in distal medium either alone (grey) or with iLM (blue). N = 3. **f**: Schematic of co-cultures of iLM with SFTPC^{TomatoTr} lineage traced adult primary alveolar epithelial type 2 (AT2) cells. **g**: Immunofluorescence images showing expression of GFP, Tomato and pro-SFTPC in primary SFTPC^{TomatoTr} lineage traced AT2 cells cultured either with iLM or with primary Pdgfra^{GFP}+ lung mesenchyme. Scale bars = 100 µm.
All bars show mean ± sd. *p<0.05, **p<0.01, ***p<0.001, ns = non-significant, as determined by paired, two-sided Student's t test.

Cross-talk between induced lung mesenchyme and epithelium in co-cultures affects mesenchymal differentiation

Finally, we sought to investigate how co-culture with Nkx2-1^{mCherry}+ cells affects the differentiation of iLM cells. Epithelial-mesenchymal interactions in lung development are thought to impact mesenchymal differentiation programs through bi-directional cross talk. However, few model systems are available to test this hypothesis in developing mammals. Supporting a critical role for the developing lung epithelium in sustaining mesenchymal cells in our model system, we observed that iLM cultured in distal differentiation medium alone showed poor survival and outgrowth (data not shown). We thus first quantified the expression of lung mesenchymal markers in iLM cells before and after co-culture in order to test whether co-culture with differentiating lung epithelial progenitors alters mesenchymal programs (Figure 7a-c). For non-lung mesenchymal controls, we quantified gene expression in MEFs after co-culture with ESC-derived Nkx2-1^{mCherry}+ (Ch+) lung epithelium. Co-culturing in distal medium with Nkx2-1^{mCherry}+ lung epithelium resulted in upregulation of *Wnt2*, *Tbx4*, *Pdgfra*, and *Acta2* uniquely in iLM, but not in MEFs, while general mesenchymal marker *Col1a1* increased in all conditions in both iLM and MEFs (Figure 7a). In contrast, lung mesenchymal progenitor marker *Foxf1* decreased. *Wnt2* is an important and relatively specific marker of both embryonic and adult lung mesenchymal

lineages in vivo[1], and these results suggest that juxtaposed developing lung epithelium in distal conditions might provide important factors to maintain and augment or mature the lung-specific identity of co-cultured iLM.

Given the upregulation of *Acta2* transcript and expression of smooth muscle actin protein (SMA, also known as ACTA2; Figure 7a-b) in iLM descendants in both distal and proximal recombinant co-cultures, we speculated that further maturation or patterning of lung mesenchyme may be occurring in our co-cultures. To explore this possibility, we first defined the in vivo global transcriptomes and cellular heterogeneity of all Acta2+ cells in the adult mouse lung at single cell resolution, using scRNA-seq to profile all GFP+ lung cells sorted from a transgenic mouse carrying bifluorescent Acta2hrGFP and Cspg4-Cre-LSL-dsRed reporters driven by promoter fragments for each gene [43] (Supplementary Figure 5a). Dimensionality reduction visualization (SPRING) as well as Louvain clustering revealed that most Acta2+ lung cells segregate into 3 main clusters, one of which expressed Notch3, as well as the dsRed lineage trace, identifying this cluster as vascular smooth muscle cells [43] (Figure 7d, Supplementary Figure 5b-c). We further compared our dataset to a previously published single cell RNA-seq dataset of adult mouse lung mesenchymal cell populations[44] and identified our 3 main clusters as Mesenchymal alveolar niche cells (MANCs), airway smooth muscle (ASM) and vascular smooth muscle cells (VSM), based on an overlay of the top 25 genes (Supplementary Table 2) found to be enriched in these 3 cell types by Zepp et al (Figure 7d). To determine whether these 3 cell types might be detectable in iLM recombinant cultures, we performed RT-qPCR of markers for each cell type in sorted iLM before and after recombinant cultures. We selected genes found among the top 30 enriched genes from our 3 in

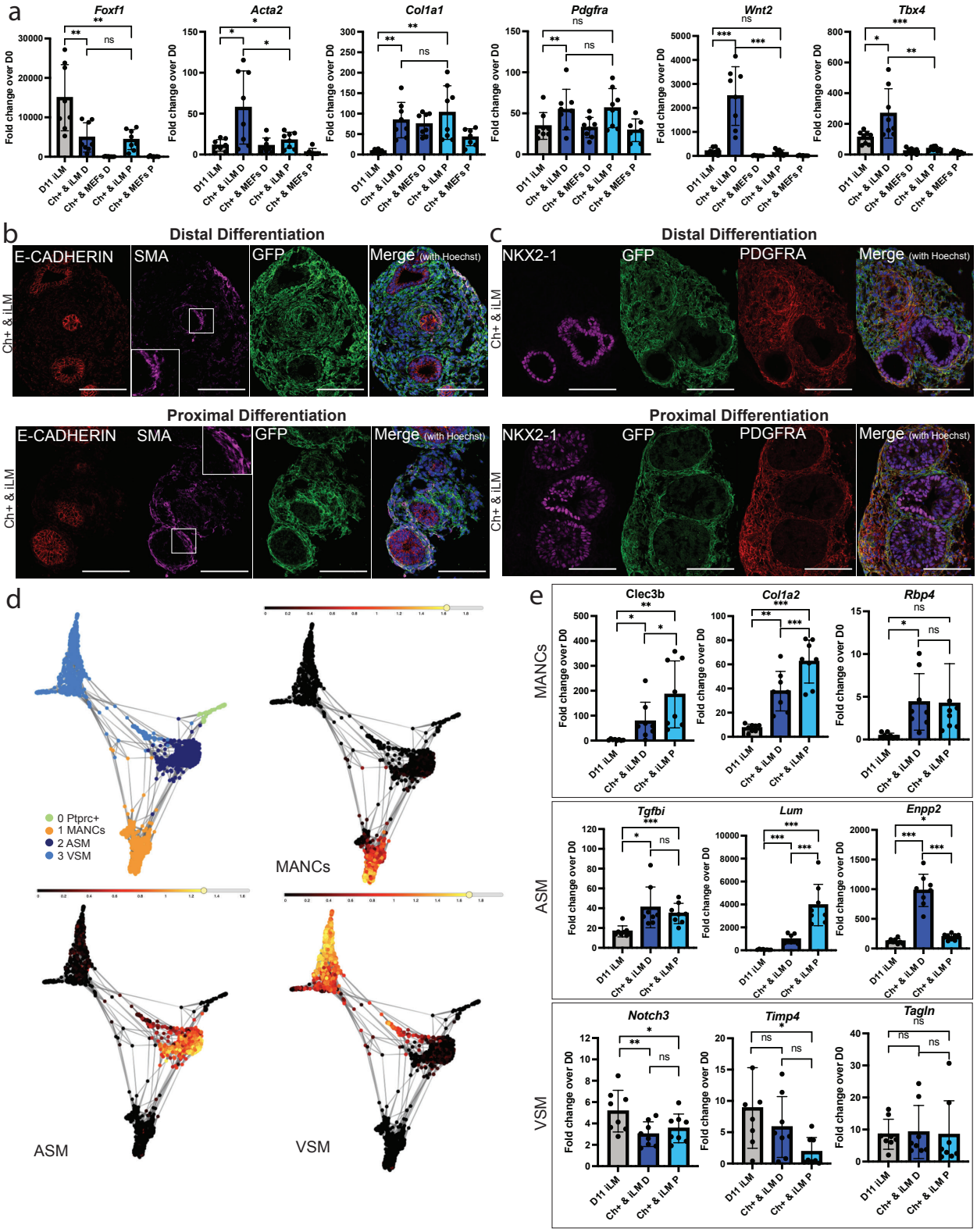

Figure 7: Cross-talk between induced lung mesenchyme and epithelium impacts mesenchymal differentiation in recombinant co-cultures.

a: RT-qPCR data showing fold change expression relative to day 0 iPSCs of lung mesenchymal markers in day 11 iLM cells before co-culture (grey), and in iLM and MEFs after co-culture in distal (dark blue) and proximal (light blue) medium.

b: Immunofluorescence images showing expression of GFP, E-CADHERIN and SMA in Nkx2-1^{mCherry}+ cells co-cultured with iLM in distal or proximal medium for 1 week. Scale bars = 100 µm. **c**: Immunofluorescence images showing expression of GFP, NKX2-1 and PDGFRA in Nkx2-1^{mCherry}+ cells co-cultured with iLM in distal or proximal medium for 1 week. Scale bars = 100 µm. **d**: SPRING plots showing Louvain clustering of mouse lung Acta2^{GFP}+ sorted cells, profiled by scRNA-seq, and overlay of gene sets for mesenchymal alveolar niche cells (MANCs), airway smooth muscle (ASM), and vascular smooth muscle (VSM) cells from Zepp et al., 2021. **e**: RT-qPCR data showing fold change expression relative to day 0 iPSCs of MANC, ASM and VSM markers in day 11 iLM cells before co-culture (grey), and in iLM after co-culture in distal (dark blue) and proximal (light blue) medium. N = 8.
All bars show mean ± sd. *p<0.05, **p<0.01, ***p<0.001, ns = non-significant, as determined by paired, two-sided Student's t test.

vivo cell clusters (Figure 7e, Supplementary Figure 5c-d, Supplementary Table 3). We also selected VSM marker Timp4, since it was found to be enriched in VSM cells in previous datasets[44,45]. Of note, most of the enriched genes selected from our mouse lung profiles were also found among the top enriched genes in Zepp et al's datasets, suggesting that these are suitable markers for each of the 3 corresponding cell types. By RT-qPCR we found that the majority of MANC and ASM markers were upregulated in iLM after recombinant culture with epithelium, both in distal and proximal media compared to pre-co-culture iLM (Figure 7e, Supplementary Figure 5d). In contrast, expression of VSM markers was either significantly decreased or unchanged (Figure 7e, Supplementary Figure 5d), suggesting that co-cultured iLM might differentiate towards airway mesenchymal and MANC-like subpopulations, but not towards vascular smooth muscle cells, consistent with the presence of alveolar/airway-like epithelial cells, but lack of vascular endothelial cells in these co-cultures.

Discussion

Our results demonstrate the directed differentiation of mouse iPSCs into functional lung-specific mesenchymal cells via KDR+ mesoderm in response to combinatorial RA and Hh signaling. Utilizing a Tbx4 enhancer element that is uniquely active in the developing lung mesenchyme of air-breathing organisms we generated a murine lineage reporter/tracer iPSC line, and used this line to optimize defined, serum-free culture conditions for the derivation of this lineage. Moreover, this reporter/tracer facilitated the quantitative tracking and purification of the derived lung-specific mesenchymal progenitors as they emerged from mesodermal precursors, further allowing their prospective isolation, functional characterization, and transcriptomic profiling at single cell resolution. Our findings significantly extend prior reports of the derivation of developing mesenchyme enriched for lung-like features[2,9]. These prior studies relied on the developing embryo as an in vivo roadmap to guide the stepwise directed differentiation in vitro of iPSCs through mesodermal precursors into specified primitive mesenchymal progenitors, some of which expressed lung-like programs.

In contrast to developing lung epithelia for which there are now a variety of validated lineage specific reporters and marker genes, developing tissue-specific mesenchymal lineages remain poorly understood, due in part to a paucity of markers available for identifying or purifying tissue-specific mesenchymal cells. While a variety of mesenchymal markers selectively distinguish mesenchymal subsets, such as fibroblasts, myofibroblasts, smooth muscle, vascular endothelium, pericytes, adipocytes, and cartilage, most of these markers tend to be expressed across a variety of organs, and little is known about the tissue-specific differences between

mesenchymal subsets across different organs, both during mesenchymal development and in the post-natal organism. We observed a variety of mesenchymal marker transcripts and gene elements expressed in our iPSC-derived mesenchyme that are also enriched in primary developing lung mesenchyme, including the Tbx4 enhancer element known to selectively identify developing lung-specific mesenchyme.

Beyond gene expression, we employed a variety of functional readouts to conclude that our derived mesenchyme appeared to be lung-like. In contrast to developing non-lung embryonic mesenchymal cells, such as MEFs, our putative lung mesenchymal progenitors augmented epithelial lung lineage specification of co-cultured foregut endodermal cells and modulated the airway and alveolar differentiation programs of their epithelial descendants. Moreover, Tbx4-LER^{GFP}+ mesenchyme after recombination with developing lung epithelia, formed spatially organized organoids with mesenchymal descendants that were closely juxtaposed to these epithelia, and expressed a variety of upregulated maturing mesenchymal programs. Most importantly, after recombination gene expression changes in both mesenchymal and epithelial lineages provided evidence of bidirectional cross-talk, a key feature of the developing lung.

Our work adds to an emerging literature focused on deriving tissue-specific mesenchymal lineages from iPSCs. In many prior studies the technique of “co-development” has been employed, where both mesenchymal and epithelial lineages are simultaneously differentiated in heterogeneous cultures that take advantage of the known inefficiencies in directed differentiation of endodermal or mesodermal germ layers[17,29]. This approach has led, in some

cases, to the formation of 3-dimensional structures containing both epithelial and mesenchymal lineages in close apposition, although whether the resulting mesenchyme was tissue-specific was not addressed[17,29]. We also attempted simultaneous co-development of mesoderm and lung endoderm, but found little evidence of lung-specific mesenchyme arising within the mesenchymal lineages that emerged in our culture conditions. In contrast, the separate derivation of putative lung-specific mesenchyme was more efficiently achieved through a dedicated mesodermal directed differentiation approach that we then optimized for the activation of the lung-mesenchymal specific reporter/tracer element through combinatorial stimulation of RA and Hh signaling. Our findings, however, only suggest that our co-development culture conditions were not optimal for lung specific mesenchymal specification compared to our dedicated mesodermal approach in our hands, and need not dissuade parallel efforts by others focused on co-development approaches for producing tissue-specific mesenchyme. Our approach of separate derivation of epithelial and mesenchymal progenitors and subsequent sorting before recombinant co-culture resulted in lung-specific identity and purity of both lineages. This approach builds on a nascent literature using separate derivation of different germ layers to engineer functional multi-lineage organoids[46]. In conclusion, we have developed an in vitro iPSC-based model system for the derivation and study of lung-specific mesenchyme with potential benefit for understanding basic mechanisms regulating tissue-specific mesenchymal fate decisions and future applications for regenerative medicine.

While engineered lung mesenchyme expressed many early lung mesenchymal markers at similar levels as primary embryonic lung mesenchyme, we did detect some differences between our

engineered cells and primary controls. In particular, expression of the important lung mesenchymal marker *Wnt2* and downstream targets of the Wnt signaling pathway were expressed at lower levels in engineered lung mesenchymal cells. Interestingly, expression of *Wnt2* significantly increased upon co-culture with lung epithelial progenitors in distal differentiation medium, suggesting that lung epithelial progenitors provide signals necessary to induce *Wnt2* expression and potentially re-enforce and improve the lung-specific identity of engineered lung mesenchymal cells. Further work will be needed to identify these signals and modify the lung mesenchyme differentiation medium accordingly in order to yield lung mesenchymal progenitors that resemble the primary control even more closely.

We have used mouse iPSCs to generate lung mesenchymal progenitors, harnessing a lung mesenchyme-specific reporter system. In order to study human lung mesenchyme development and to model human respiratory diseases involving the mesenchymal lineage, such as pulmonary fibrosis, establishing a protocol for the differentiation of human iPSCs into lung mesenchyme will be crucial. The *Tbx4* lung enhancer region is highly conserved in mouse and humans, however, it is unclear if this enhancer activates in the same lung-mesenchyme specific manner as in the mouse. Future work can focus on testing a human reporter and adapting our approach for the derivation of human lung-specific mesenchyme from patient-specific iPSCs.

Methods

Generation and maintenance mouse iPSC/ESC lines

A Tbx4-LER reporter/tracer iPSC line was generated by reprogramming tail tip fibroblasts from adult Tbx4-LER triple transgenic mice carrying an rtTA/LacZ encoding cassette under regulatory control of a Tbx4 lung-specific enhancer, a Tet-responsive Cre recombinase, and a fluorescent mTmG cassette (Tbx4-rtTA; TetO-Cre; mTmG, hereafter "Tbx4-LER")[34]. Reprogramming was performed as previously published [24] using an excisable lentiviral STEMCCA-Frt vector followed by vector excision with transient flipase expression (adeno-flp)[24] as shown in Supplementary Figure 1. A normal karyotype was documented by G-banding analysis (Cell Line Genetics). For lung epithelial differentiation, a Nkx2-1^{mCherry} reporter ESC line[40] was differentiated using protocols we have previously published for this line[27]. All iPSC/ESC lines were maintained on mouse embryonic fibroblasts in medium containing DMEM with 15% ESC-qualified fetal bovine serum (ThermoFisher, 16141061), Glutamax (Life Technologies, 35050-061), 0.1 mM Beta-mercaptoethanol (Fisher Scientific, #21985-023), Primocin (Fisher Scientific, NC9141851) and Leukemia inhibitory factor.

Animal maintenance and isolation of E12.5 mouse embryonic lung mesenchyme

All experiments involving mice were approved by the Institutional Animal Care and Use Committee of Boston University School of Medicine. For the isolation of primary mouse embryonic tissue (C57BL/6J strain) on embryonic day (E)12.5 pregnant female mice were euthanized and embryonic lungs were isolated using Tungsten needles (Fine Science Tools, #10130-10) and kept in HBSS with 10% FBS on ice. Lungs were subsequently single cell digested

using TrypLE (Gibco, #12640-013) for 15 min at 37 °C. Cells were treated with Red Blood Cell Lysing Buffer (Sigma, #R7767) and incubated with an anti CD326 antibody (BD Biosciences, # 563214, 1/500) for 30 min on ice. Lung mesenchyme and epithelium were isolated by fluorescence activated cell sorting (FACS) for Epcam- versus Epcam+ cells. For co-cultures of iLM with adult alveolar epithelial type 2 (AT2) cells, primary AT2 cells were isolated based on flow cytometry sorting tdTomato+ lineage traced cells from single cell suspensions prepared from the lungs of adult (3-6 month old) mice carrying knock-in Sftpc-CreER^{T2} and Rosa-tdTomato alleles [42]. For control primary-primary co-cultures, a Pdgfra^{GFP} reporter mouse line was used[47]. For isolation of adult Acta2+ lung cells, a previously published Acta2hrGFP/Cspg4-Cre-LSL-dsRed bifluorescent mouse line was used[43] and GFP+ live cells were sorted from lung digested single cell suspensions for scRNA-seq profiling.

Directed differentiation of iPSCs into lung mesenchyme

Tbx4-LER iPSCs were first differentiated into lateral plate mesoderm as previously published[35]. In brief, iPSCs were trypsinized and subsequently depleted of MEFs by incubating in 10-cm tissue culture dishes (Fisher Scientific, #FB012924) in ESC medium at 37 °C for 30 mins to let MEFs attach. Remaining iPSCs in medium were collected by centrifugation at 300*x*g for 5 min. 1.5 x 10^6 cells were plated in 10-cm non-adherent Petri dishes (Fisher Scientific, #FB0875712) in complete serum-free differentiation medium (cSFDM). 500 ml cSFDM was composed of 375 ml IMDM (ThermoFisher, #12440053), 125 ml Ham's F12 (Cellgro, #10-080-CV), 5 ml Glutamax 100x (Invitrogen, #35050-061), 5 ml B27 supplement without vitamin A (Invitrogen, #12587-010), 2.5 ml N2 (Invitrogen, #17502-048), 3.3 ml 7.5% BSA (Life Technologies, #15260-037), 19.5 µL 1-

thioglycerol (final concentration 4.5 x 10-4 M, Sigma, #M6145), 500 µl ascorbic acid (final concentration 50 µg/ml, Sigma, #A4544), and 1 ml Primocin (final concentration 100 µg/ml, Fisher Scientific, #NC9392943). Cells were incubated at 37 °C for 48 h to allow embryoid bodies to form. Embryoid bodies were then collected by gravity, re-plated and incubated in 10-cm non-adherent Petri dishes in cSFDM containing 2 ng/ml rhActivin A (R&D Systems, #338-AC), 3 ng/ml rhBMP4 (R&D Systems, #314-BP), and 3 ng/ml rmWNT3a (R&D Systems, #1324-WN-010) for 72 hours. Day 5 mesodermal progenitors were then collected by gravity. For assessment of mesodermal differentiation efficiency, a small subset of embryoid bodies was removed, single cell dispersed by 0.05% trypsin, and incubated in anti-FLK1 (i.e. anti KDR) antibody (anti-FLK1; BD Biosciences, #560070, 1/50) or Isotype (BD Biosciences, # 553932) for 30 min on ice. Cells were then stained with live/dead Calcein Blue (Life Technologies, #C1429) and analyzed by flow cytometry using a Stratedigm flow cytometer. For subsequent differentiation into lung mesenchyme, the remaining mesodermal progenitors were plated without enzymatic digestion on gelatin-coated (Stemcell Technologies, #07903) 12-well plates at an approximate cell density of 40,000 cells/cm^2 in cSFDM with 2 µM Retinoic acid (Sigma, #R2625). From day 7 - 9 of differentiation cells were cultured in cSFDM containing 2 µM Retinoic acid and 0.5 µg/ml purmorphamine (Stemcell Technologies, #72202), and then subsequently in cSFDM with 2 µM Retinoic acid until day 11-13 of differentiation. For the initial media screen (See Figure 1e), 3ng/ml rmWNT3a (R&D Systems, #1324-WN-010) and/or 3 ng/ml rhBMP4 (R&D Systems, #314-BP) was also added to the medium from day 5 – 13, but rmWNT3A and rhBMP4 were not included in the day 5-13 medium in all subsequent experiments. 2 µg/ml Doxycycline (Sigma, #D3072) was added to the medium from day 5-13, or day 9-11, as indicated in the main text and figure legends.

For analysis/sorting, cells were single cell dispersed by 0.05% trypsin and stained with live/dead Calcein Blue. Tbx4-LER^{GFP} percentage was quantified using a Stratedigm flow cytometer. Sorting was performed at the BU Flow Cytometry Core Facility using a MoFlo sorter.

Directed differentiation of lung mesenchyme into more mature mesenchymal lineages

For smooth muscle differentiation, day 13 GFP+/cells were sorted and plated on gelatin-coated 12well plates at a density of 40,000 cells/cm^2 and cultured in our previously published smooth muscle differentiation medium[35], consisting of cSFDM with 10 ng/ml rhPDGF-BB (Life Technologies, #PHG0046), 10 ng/mL rmTGF-β (R&D Systems, #7666-MB-005), and 10 ng/mL rhFGF2 (R&D Systems, #233-FB) for 4 days. Cells were harvested for RNA extraction, and differentiation efficiency was evaluated by RT-qPCR for the smooth muscle markers *Acta2* and *Tagln*.

For adipogenic differentiation, day 13 GFP+ cells were sorted, plated on gelatin-coated glass chamber slides (Millipore, #PEZGS0816) at a density of 40,000 cells/cm^2 and cultured in MesenCult Adipogenic differentiation medium (Stemcell Technologies, #05507), or cSFDM containing 2 µM Retinoic acid (control) for 9 days. Cells were then fixed in 4 % paraformaldehyde for 30 min at room temperature and stained with hematoxylin and Oil Red O (Sigma, #O0625) to visualize nuclei and lipid droplets. Chambers were subsequently removed, slides were mounted and imaged using a Keyence BZ-X700 fluorescence microscope.

For endothelial differentiation, day 5 lateral plate mesoderm or day 7 differentiating lung mesenchyme was transferred to cSFDM supplemented with 100 ng/ml rmVEGF (R&D Systems, # 493-MV-005). For evaluation of differentiation efficiency, cells were dispersed into a single cell

suspension using 0.05 % trypsin and subsequently incubated with an anti CD144 antibody (anti-VE-Cadherin; BD Biosciences, #562242, 1/50) for 30 min on ice. Cells were stained with the live/dead Calcein Blue and analyzed by flow cytometry using a Stratedigm flow cytometer.

Directed differentiation of iPSCs/ESCs into lung epithelial progenitors

For lung epithelial differentiation, iPSCs/ESCs were MEF-depleted and differentiated according to our previously published serum-free protocol[27,37]. On day 13, cells were harvested by incubating in 2 mg/ml Dispase (Gibco, #17105-041) for 1.5 h at 37 °C, 2x centrifugation for 2 min at 50*x*g, and subsequent single cell dispersion by 0.05 % trypsin. Cells were then stained for Epcam using an anti CD326 antibody (BD Biosciences, # 563214, 1/500) and the live/dead stain DRAQ7 (Biolegend, #424001, 1/100 dilution). Sorting for Epcam+, Nkx2-1^{mCherry}+ or GFP+ cells, as indicated in the text, was performed at the BU Flow Cytometry Core Facility using a MoFlo sorter.

Co-culture of engineered lung epithelial and mesenchymal cells

For epithelial-mesenchymal co-cultures, 24- or 48 well tissue culture plates were coated with a layer of 3D Matrigel and incubated at 37 °C for 20 min to let the Matrigel solidify. Day 13 Nkx2-1^{mCherry}+/- cells were then combined with sorted day 11 Tbx4-LER^{GFP}+ cells or MEFs (control) at a 1/20 epithelial/mesenchymal cell ratio and seeded in the Matrigel coated plates at a density of 110 000 cells/cm^2. For co-cultures with primary AT2 cells, Sftpc^{TomatoTr}+ lineage traced cells were isolated from adult mouse lungs and combined with day 11 Tbx4-LER^{GFP}+ or freshly isolated Pdgfra^{GFP}+ primary lung mesenchymal cells and plated on Matrigel coated plates. For distal epithelial differentiation, cells were incubated in cSFDM (including B27 supplement with vitamin

A) with 200 ng/ml rmWNT3A (R&D Systems, #1324-WN-010), 100 ng/ml rhFGF2 (R&D Systems, #233-FB), 100 ng/ml rhFGF10 (R&D Systems, # 345-FG), and 10 µM Y-27632 (Tocris, #1254). For proximal epithelial differentiation, cells were incubated in cSFDM (with RA-containing B27 supplement) with 100 ng/ml rhFGF2 (R&D Systems, #233-FB), 100 ng/ml rhFGF10 (R&D Systems, # 345-FG), 100 ng/ml Heparin Salt (Millipore Sigma, #H3393), and 10 µM Y-27632 (Tocris, #1254). In the distal differentiation medium, Y-27632 was removed after 48 h. Distal and proximal differentiation media were exchanged every 48 h for 7 days. Day 7 co-cultures were imaged using a Keyence BZ-X700 fluorescence microscope. In order to re-separate co-cultured cells for sorting and RT-qPCR analysis, Matrigel was disrupted by incubating in 2mg/ml Dispase for 1.5 h at 37 °C. Cells were then harvested by centrifugation at 300*x*g for 5 min, single cell dispersed by 0.05 % trypsin, and stained for Epcam using an anti-CD326 antibody (BD Biosciences, # 563214, 1/500 dilution) and the live/dead stain DRAQ7 (Biolegend, #424001, 1/100 dilution). Sorting was performed at the BU Flow Cytometry Core Facility using a MoFlo sorter. Upon gating for single and live cells, Nkx2-1^{mCherry}+ cells were isolated by further sorting for Epcam+/mCherry+ cells, Tbx4-LER^{GFP}+ cells were isolated by sorting for Epcam-/GFP+ cells, and MEFs were isolated by sorting for Epcam-/mCherry- cells. Harvested cells were resuspended in Qiazol Lysis reagent (Qiagen, #79306) and stored at -80 °C for further analysis.

Reverse Transcriptase Quantitative Real Time Polymerase Chain Reaction (RT-qPCR)

RNA was extracted using an RNeasy Plus Mini Kit (QIAGEN, #74136) according to the manufacturer's instructions. RNA was eluted in 30 µl nuclease-free water and quantified using a NanoDrop ND-1000 microvolume spectrophotometer (ThermoFisher Scientific, Waltham, MA).

cDNA was generated from 150 ng of RNA in a 20 µl reaction using a High-Capacity cDNA Reverse Transcription Kit (Applied Biosystems, #4368814). qPCR was performed using TaqMan Fast Universal PCR Master Mix (ThermoFisher, #364103). cDNA was diluted 1/16 and 4 µl of diluted cDNA was used in a 10 µl qPCR reaction, using an Applied Biosystems QuantStudio7 384-well System. Relative expression was calculated using the the $2^{(-\Delta\Delta Ct)}$ method [48], using 18S rRNA (ThermoFisher, #4318839) as the internal reference gene and undifferentiated (day 0) iPSCs as the reference sample. Undetected Ct values were set to the maximum number of cycles (40) to allow fold change calculations. TaqMan gene expression arrays were purchased from ThermoFisher.

Embedding of organoids and immunofluorescence experiments

In order to allow for fixation and paraffin embedding, lung epithelial-mesenchymal co-cultures were plated on glass chamber slides (Millipore, #PEZGS0816) coated with 3D Matrigel. On day 7 of co-culture, medium was removed from the chambers and another layer of 3D Matrigel was added on top of the co-cultures and allowed to solidify at 37 °C for 20 min. Chambers were removed from the slides and Matrigel pellets containing lung epithelial-mesenchymal organoids were carefully removed, transferred to 12 well plates, and incubated in 4% paraformaldehyde for 1 h at room temperature. Samples were washed, dehydrated, and paraffin-embedded. 5 µm sections were de-paraffinized and treated with citric acid-based Antigen Unmasking Solution (Vector Laboratories, #H-3300) according to the manufacturer's instructions. After washing in PBS and blocking with 10% Normal Donkey Serum (Sigma, #D9663), 2% BSA (Fisher Scientific, #BP1600), and 0.5% TritonX-100 (Sigma) for 1 h at room temperature, sections were incubated

in primary antibody (chicken anti-GFP, Aves labs GFP-1010, 1/500; goat anti-PDGFRA, R&D Systems AF1062, 1/200; rat anti-SOX2, ThermoFisher 14-9811-82, 1/250; rat anti-E-cadherin, Invitrogen 13-1900, 1/200; rabbit anti-SMA, Abcam ab5694, 1/500; rabbit anti-proSFTPC, Abcam ab211326, 1/250; rabbit anti-SOX9, Abcam ab185966, 1/500; rabbit anti-TTF1 (Nkx2-1), Abcam ab76013, 1/500; rabbit anti-p63, Cell Signaling 13109, 1/500) resuspended in ¼ blocking buffer over night at 4 °C, washed 3 x with PBS, and incubated in secondary antibody (1/500) and Hoechst 33342 (ThermoFisher, # H3570, 1/500) for 2 h at room temperature. Slides were subsequently washed 1x with PBS and mounted using FluorSave mounting reagent (Millipore, # 345789). Slides were imaged using a Zeiss LSM710 confocal microscope.

Single cell RNA sequencing

For scRNA-seq of iPSC-derived and primary lung mesenchymal cells, Tbx4-LER iPSCs were differentiated into lung mesenchyme using the directed differentiation protocol described above, and subsequently sorted for Tbx4-LER^{GFP}+ and Tbx4-LER^{GFP}- cells. In parallel, to generate co-developed lung mesenchyme Tbx4-LER iPSCs were differentiated using the lung epithelium protocol as described above, stained with Epcam antibody (anti-CD326, BD Biosciences, # 563214, 1/500), and sorted for Tbx4-LER^{GFP}+ (cLM) cells and Epcam+/Tbx4-LER^{GFP}- (i.e. epithelial) cells. cLM and epithelial cells were mixed at a 3:1 ratio. For primary controls, primary embryonic lungs from embryonic day E12.5 were isolated and single cell digested as described above, stained with Epcam antibody (anti-CD326 antibody, BD Biosciences, # 563214, 1/500), and sorted for Epcam- and Epcam+ cells. Epcam- and Epcam+ cells were mixed at a 3:1 ratio. For the single cell RNA-seq of adult mouse Acta2+ cells, GFP+ live cells were sorted from adult

Acta2hrGFP/Cspg4-Cre-LSL-dsRed mice[43]. All sorts were performed at the BU Flow Cytometry Core Facility using a MoFlo sorter and cells were resuspended in FACS buffer at a concentration of 1000 cells/µl. Single cell capture (10X Chromium instrument; 10X Genomics, Pleasanton, CA), library preparation (Chromium Single-Cell 30 Library Kit; 10X Genomics), and sequencing was performed at the Boston University Single Cell Sequencing Core Facility. Sequencing libraries were loaded on a NextSeq500 (Illumina) with a custom sequencing setting to obtain a sequencing depth of ~40k reads/cell. The average sample had a mean of 56,451 reads per cell (ranging from 49,239 to 61,912 depending on the sample.). The median number of genes detected per cell on the average sample was 3793 genes. The UMI count matrix was further processed with Seurat v. 3.1.0[49]. As part of the quality control, we filtered out stressed and dead cells (those with high percentages of reads mapping to mitochondrial genes, using manually curated thresholds based on the shape of the distribution) and removing potential doublets (barcodes with a number of genes detected beyond the percentile that would be expected at a given cell density per library, based on 10X Chromium Assay reports). After normalization with SCTransform, scaling and correcting for unwanted sources of variation (like cell degradation), we identified highly variable genes and used them for linear dimensionality reduction (with Principal Component Analysis). The top 40 principal components were then used to build the KNN graph and Louvain clustering at different resolutions. Further non-linear dimensionality reduction was performed with SPRING[50]. For computational analysis of iPSC-derived Tbx4-LER^{GFP}+/- versus primary lung mesenchyme, Louvain clustering with a resolution of 0.1 was used, and epithelial and other non-mesenchymal (i.e. endothelial, immune cell) clusters were removed for further analysis. Tbx4-LER^{GFP}+ cells from the mesenchymal differentiation, Tbx4-LER^{GFP}- cells from the mesenchymal

differentiation, and cLM cells clustered separately, and primary cells formed 2 distinct clusters, one of which was annotated as a mesothelial cluster based on the top 50 enriched genes and expression of known mesothelial markers genes such as *Wt1*. The Cell Ranger pipeline was used to identify the top 50 DEGs in each cluster, represented as a heatmap (Supplementary Figure 2). For computational analysis of single cell RNA-seq of adult Acta2+ lung cells, Louvain clustering with a resolution of 0.25 was used, and clusters were annotated as MANCs, ASM and VSM based on enrichment of gene sets identified by Zepp et al, 2021 (detailed in Supplementary Table 2). An additional minor cell cluster was presumed to be non-mesenchymal hematopoietic cells based on expression of the pan-hematopoietic marker, *Ptprc* (CD45).

Statistical analysis

All bar graphs represent mean and standard deviation. Number of biological replicates for RT-qPCR/flow cytometry analysis are indicated in the figure legends, at least 3 replicates were used for all experiments. Statistically significant differences between conditions were determined using two-tailed unpaired or paired Student's t test, as indicated in the figure legends. Statistical significance was defined as $p<0.05$, $^{**}p<0.01$, $^{***}p<0.001$.

Data Availability

The scRNA-seq data reported in this publication have been deposited in NCBI's Gene Expression Omnibus. The accession number for the scRNA-seq dataset comparing engineered to primary embryonic lung mesenchyme is GSE203245. The accession number for the scRNA-seq dataset focusing on mouse lung Acta2+ cells is GSE203243.

References

1. Goss, A. M. *et al.* Wnt2/2b and β-Catenin Signaling Are Necessary and Sufficient to Specify Lung Progenitors in the Foregut. *Developmental Cell* **17**, 290–298 (2009).
2. Han, L. *et al.* Single cell transcriptomics identifies a signaling network coordinating endoderm and mesoderm diversification during foregut organogenesis. *Nat Commun* **11**, 4158 (2020).
3. Han, L., Nasr, T. & Zorn, A. M. Mesodermal lineages in the developing respiratory system. *Trends Dev Biol* **9**, 91–110 (2016).
4. Rankin, S. A. & Zorn, A. M. Gene Regulatory Networks Governing Lung Specification: Lung Specification GRN. *J. Cell. Biochem.* **115**, 1343–1350 (2014).
5. Bellusci, S., Henderson, R., Winnier, G., Oikawa, T. & Hogan, B. L. Evidence from normal expression and targeted misexpression that bone morphogenetic protein (Bmp-4) plays a role in mouse embryonic lung morphogenesis. *Development* **122**, 1693–1702 (1996).
6. Cardoso, W. V., Mitsialis, S. A., Brody, J. S. & Williams, M. C. Retinoic acid alters the expression of pattern-related genes in the developing rat lung. *Dev. Dyn.* **207**, 47–59 (1996).
7. Chen, F. *et al.* Prenatal retinoid deficiency leads to airway hyperresponsiveness in adult mice. *J. Clin. Invest.* **124**, 801–811 (2014).
8. Harris-Johnson, K. S., Domyan, E. T., Vezina, C. M. & Sun, X. beta-Catenin promotes respiratory progenitor identity in mouse foregut. *Proc Natl Acad Sci U S A* **106**, 16287–16292 (2009).

9. Kishimoto, K. *et al.* Bidirectional Wnt signaling between endoderm and mesoderm confers tracheal identity in mouse and human cells. *Nat Commun* **11**, 4159 (2020).
10. Litingtung, Y., Lei, L., Westphal, H. & Chiang, C. Sonic hedgehog is essential to foregut development. *Nat Genet* **20**, 58–61 (1998).
11. Pepicelli, C. V., Lewis, P. M. & McMahon, A. P. Sonic hedgehog regulates branching morphogenesis in the mammalian lung. *Current Biology* **8**, 1083–1086 (1998).
12. Rankin, S. A. *et al.* A Retinoic Acid-Hedgehog Cascade Coordinates Mesoderm-Inducing Signals and Endoderm Competence during Lung Specification. *Cell Reports* **16**, 66–78 (2016).
13. Shu, W., Jiang, Y. Q., Lu, M. M. & Morrisey, E. E. Wnt7b regulates mesenchymal proliferation and vascular development in the lung. *Development* **129**, 4831–4842 (2002).
14. Yin, Y. *et al.* An FGF–WNT gene regulatory network controls lung mesenchyme development. *Developmental Biology* **319**, 426–436 (2008).
15. Ebert, A. D., Liang, P. & Wu, J. C. Induced Pluripotent Stem Cells as a Disease Modeling and Drug Screening Platform: *Journal of Cardiovascular Pharmacology* **60**, 408–416 (2012).
16. Snoeck, H.-W. Modeling human lung development and disease using pluripotent stem cells. *Development* **142**, 13–16 (2015).
17. Dye, B. R. *et al.* In vitro generation of human pluripotent stem cell derived lung organoids. *eLife* **4**, e05098 (2015).
18. Gotoh, S. *et al.* Generation of Alveolar Epithelial Spheroids via Isolated Progenitor Cells from Human Pluripotent Stem Cells. *Stem Cell Reports* **3**, 394–403 (2014).

19. Green, M. D. *et al.* Generation of anterior foregut endoderm from human embryonic and induced pluripotent stem cells. *Nat Biotechnol* **29**, 267–272 (2011).

20. Hawkins, F. *et al.* Prospective isolation of NKX2-1–expressing human lung progenitors derived from pluripotent stem cells. *Journal of Clinical Investigation* **127**, 2277–2294 (2017).

21. Hawkins, F. J. *et al.* Derivation of Airway Basal Stem Cells from Human Pluripotent Stem Cells. *Cell Stem Cell* **28**, 79-95.e8 (2021).

22. Huang, S. X. L. *et al.* Efficient generation of lung and airway epithelial cells from human pluripotent stem cells. *Nat Biotechnol* **32**, 84–91 (2014).

23. Jacob, A. *et al.* Differentiation of Human Pluripotent Stem Cells into Functional Lung Alveolar Epithelial Cells. *Cell Stem Cell* **21**, 472-488.e10 (2017).

24. McCauley, K. B. *et al.* Single-Cell Transcriptomic Profiling of Pluripotent Stem Cell-Derived SCGB3A2+ Airway Epithelium. *Stem Cell Reports* **10**, 1579–1595 (2018).

25. McCauley, K. B. *et al.* Efficient Derivation of Functional Human Airway Epithelium from Pluripotent Stem Cells via Temporal Regulation of Wnt Signaling. *Cell Stem Cell* **20**, 844-857.e6 (2017).

26. Mou, H. *et al.* Dual SMAD Signaling Inhibition Enables Long-Term Expansion of Diverse Epithelial Basal Cells. *Cell Stem Cell* **19**, 217–231 (2016).

27. Serra, M. *et al.* Pluripotent stem cell differentiation reveals distinct developmental pathways regulating lung- versus thyroid-lineage specification. *Development* **144**, 3879–3893 (2017).

28. Yamamoto, Y. *et al.* Long-term expansion of alveolar stem cells derived from human iPS cells in organoids. *Nat Methods* **14**, 1097–1106 (2017).

29. Chen, Y.-W. *et al.* A three-dimensional model of human lung development and disease from pluripotent stem cells. *Nat Cell Biol* **19**, 542–549 (2017).

30. Ng, W. H. *et al.* Recapitulating human cardio-pulmonary co-development using simultaneous multilineage differentiation of pluripotent stem cells. *Elife* **11**, e67872 (2022).

31. Shannon, J. M. Induction of Alveolar Type II Cell Differentiation in Fetal Tracheal Epithelium by Grafted Distal Lung Mesenchyme. *Developmental Biology* **166**, 600–614 (1994).

32. Menke, D. B., Guenther, C. & Kingsley, D. M. Dual hindlimb control elements in the Tbx4 gene and region-specific control of bone size in vertebrate limbs. *Development* **135**, 2543–2553 (2008).

33. Kumar, M. E. *et al.* Defining a mesenchymal progenitor niche at single-cell resolution. *Science* **346**, 1258810–1258810 (2014).

34. Zhang, W. *et al.* Spatial-temporal targeting of lung-specific mesenchyme by a Tbx4 enhancer. *BMC Biol* **11**, 111 (2013).

35. Kwong, G., Marquez, H. A., Yang, C., Wong, J. Y. & Kotton, D. N. Generation of a Purified iPSC-Derived Smooth Muscle-like Population for Cell Sheet Engineering. *Stem Cell Reports* **13**, 499–514 (2019).

36. Gadue, P., Huber, T. L., Paddison, P. J. & Keller, G. M. Wnt and TGF-beta signaling are required for the induction of an in vitro model of primitive streak formation using embryonic stem cells. *Proceedings of the National Academy of Sciences* **103**, 16806–16811 (2006).

37. Ikonomou, L. *et al.* The in vivo genetic program of murine primordial lung epithelial progenitors. *Nat Commun* **11**, 635 (2020).

38. Bellusci, S., Grindley, J., Emoto, H., Itoh, N. & Hogan, B. L. Fibroblast growth factor 10 (FGF10) and branching morphogenesis in the embryonic mouse lung. *Development* **124**, 4867–4878 (1997).

39. Min, H. *et al.* Fgf-10 is required for both limb and lung development and exhibits striking functional similarity to Drosophila branchless. *Genes & Development* **12**, 3156–3161 (1998).

40. Bilodeau, M., Shojaie, S., Ackerley, C., Post, M. & Rossant, J. Identification of a Proximal Progenitor Population from Murine Fetal Lungs with Clonogenic and Multilineage Differentiation Potential. *Stem Cell Reports* **3**, 634–649 (2014).

41. Barkauskas, C. E. *et al.* Type 2 alveolar cells are stem cells in adult lung. *J. Clin. Invest.* **123**, 3025–3036 (2013).

42. Rock, J. R. *et al.* Multiple stromal populations contribute to pulmonary fibrosis without evidence for epithelial to mesenchymal transition. *Proc. Natl. Acad. Sci. U.S.A.* **108**, (2011).

43. Paez-Cortez, J. *et al.* A New Approach for the Study of Lung Smooth Muscle Phenotypes and Its Application in a Murine Model of Allergic Airway Inflammation. *PLoS ONE* **8**, e74469 (2013).

44. Zepp, J. A. *et al.* Genomic, epigenomic, and biophysical cues controlling the emergence of the lung alveolus. *Science* **371**, eabc3172 (2021).

45. Zepp, J. A. *et al.* Distinct Mesenchymal Lineages and Niches Promote Epithelial Self-Renewal and Myofibrogenesis in the Lung. *Cell* **170**, 1134-1148.e10 (2017).

46. Eicher, A. K. *et al.* Functional human gastrointestinal organoids can be engineered from three primary germ layers derived separately from pluripotent stem cells. *Cell Stem Cell* **29**, 36-51.e6 (2022).

47. Hamilton, T. G., Klinghoffer, R. A., Corrin, P. D. & Soriano, P. Evolutionary Divergence of Platelet-Derived Growth Factor Alpha Receptor Signaling Mechanisms. *Mol Cell Biol* **23**, 4013–4025 (2003).

48. Livak, K. J. & Schmittgen, T. D. Analysis of relative gene expression data using real-time quantitative PCR and the 2(-Delta Delta C(T)) Method. *Methods* **25**, 402–408 (2001).

49. Stuart, T. *et al.* Comprehensive Integration of Single-Cell Data. *Cell* **177**, 1888-1902.e21 (2019).

50. Weinreb, C., Wolock, S. & Klein, A. M. SPRING: a kinetic interface for visualizing high dimensional single-cell expression data. *Bioinformatics* **34**, 1246–1248 (2018).

Acknowledgements

The authors wish to thank all members of the Kotton lab for insightful discussions. We thank Brian R Tilton from the Boston University Flow Cytometry Core Facility for cell sorting, Yuriy Alekseyev, Katerina Zhang, and Ashley LeClerc of the Boston University School of Medicine (BUSM) Single Cell Sequencing Core for RNA sequencing, and Hui Chen and Joanne Chiu for help with mouse work. This work was supported by the Swiss National Science Foundation (P2ELP3_191217 and P500PB_206631 to A.B.A.) and the U.S. National Institutes of health (U01HL134745, U01HL134766, U01HL152976, and R01HL095993 to D.N.K., R01HL141352 and R01HL146541 to W.S., and R56 DE028545-01 to L.I.). L.I. was also supported by University at Buffalo (UB) Research Foundation Start-up Funds. Schematics were created with BioRender.com.

Author contributions

Conceptualization and Methodology, D.N.K., A.B.A and H.A.M. Investigation and analysis, A.B.A., H.A.M., L.M., G.K., B.R.T., Y.L. and L.I. Software C.V-M., J.L.-V. and P.B. Resources, W.S. Visualization and Writing, A.B.A. and D.N.K. Supervision, D.N.K.

Competing interests

The authors declare no competing interests.

Materials & Correspondence

Correspondence and requests for material should be addressed to D.N.K.